

ULSLEA v2.0 January 1996
Manual v1.0 June 1996

ULSLEA v2.0
Ultimate Limit State Limit Equilibrium Analysis
Merhdad Mortazavi and Professor Robert G. Bea

ULSLEA Manual v1.0
James D. Stear, Mehrdad Mortazavi, and Professor Robert G. Bea

This software and manual is provided "as is" by the Marine Technology and Management Group (MTMG) at University of California at Berkeley to sponsors of the research project "Screening Methodologies for Use in Platform Assessments and Requalifications." Any express or implied warranties of merchantability and fitness for a particular purpose are disclaimed. In no event shall the MTMG be liable for any direct, indirect, incidental, special, exemplary, or consequential damages (including, but not limited to, procurement of substitute goods or services; loss of use, data, or profits; or business interruption) however caused on any theory of liability, whether in contract, strict liability, or tort (including negligence or otherwise) arising in any way out of the use of this software, even if advised of possibility of such damage.

ULSLEA v2.0 is password protected. The password to access the program, and to unlock and edit its executable code, is "ULSLEAMTMG".

Table of Contents

1.0	INTRODUCTION	1-1
1.1	Program Overview	1-2
1.2	How to Use this Manual/Getting Started	1-2
1.3	Scope of Application and Limitations	1-3
1.4	Acknowledgments	1-3
2.0	ANALYSIS METHODOLOGY	2-1
2.1	Overview of Program Operation	2-2
2.2	Environmental Load Formulation	2-7
2.2.1	Wind Loads	2-7
2.2.2	Wave Loads	2-7
2.3	Ultimate Strength of Platform Components	2-10
2.3.1	Deck Bay	2-10
	Deck Bay Drift at Collapse	2-11
	Deck Legs Lateral Shear Strength	2-12
2.3.2	Jacket Bays	2-12
	Ultimate Axial Strength of Tubular Braces	2-13
	Effect of Shear Force in Jacket Legs and Piles	2-15
	Jacket Bays Lateral Shear Strength	2-17
2.3.3	Ultimate Strength of Tubular Joints	2-18
2.3.4	Foundation Bay	2-19
	Ultimate Lateral Strength of Pile Foundations	2-19
	Ultimate Axial Strength of Pile Foundations	2-23
2.3.5	Damaged and Grout-Repaired Members	2-25
	Dents and Global Bending Damage (Loh's Interaction Equations)	2-25
	Corrosion Damage	2-26
	Grout-Repaired Tubular Members (Parsanejad Method)	2-26
2.4	Reliability Analysis	2-33
	Component Reliability	2-33
	Loading Formulation	2-35
	Capacity Formulation: Deck Leg's Shear Capacity	2-36
	Capacity Formulation: Jacket Bays' Shear Capacity	2-37
	Capacity Formulation: Foundation	2-39
2.5	Preliminary Design	2-40
2.6	References	2-41
3.0	PROGRAM INSTALLATION	3-1
3.1	Hardware and Software Requirements	3-2
3.2	Installing ULSLEA	3-2
4.0	ULSLEA TUTORIAL	4-1
4.1	Starting the Program	4-1

4.2	Main Menus	4-3
4.3	Inputting Data	4-4
4.3.1	Preliminary Design	4-5
4.3.2	Environmental Conditions	4-5
4.3.3	Global Parameters	4-6
4.3.4	Local Parameters	4-9
	Decklegs and Vertical Diagonal Braces	4-10
	Horizontal Braces	4-12
	Joints	4-12
	Foundation	4-13
	Force Coefficients	4-13
	Boatlandings and Appurtenances	4-14
4.3.5	Member Strength, Material and Soil Properties	4-15
4.3.6	Uncertainties and Biases	4-16
4.4	Calculation	4-17
4.5	Output	4-17
4.6	Saving and Quitting	4-21

Appendix A: Example Application (PMB Benchmark Platform)

Appendix B: Errors and Warnings

1.0 INTRODUCTION

Contents:

1.1	Program Overview	1-2
1.2	How to Use this Manual/Getting Started	1-2
1.3	Scope of Application and Limitations	1-3
1.4	Acknowledgments	1-3

2.0 ANALYSIS METHODOLOGY

This chapter provides the user with a detailed description of the mechanics and assumptions which are utilized by ULSLEA when performing a structural evaluation. The development and verification of ULSLEA has been thoroughly documented by Mortazavi and Bea (1996); users desiring further information or verification of the operating assumptions of the program are referred to that document.

Contents:

2.1	Overview of Program Operation	2-2
2.2	Environmental Load Formulation	2-7
2.2.1	Wind Loads	2-7
2.2.2	Wave and Current Loads	2-7
2.3	Ultimate Strength of Platform Components	2-10
2.3.1	Deck Bay	2-10
	Deck Bay Drift at Collapse	2-11
	Deck Legs Lateral Shear Strength	2-12
2.3.2	Jacket Bays	2-12
	Ultimate Axial Strength of Tubular Braces	2-13
	Effect of Shear Force in Jacket Legs and Piles	2-15
	Jacket Bays Lateral Shear Strength	2-17
2.3.3	Ultimate Strength of Tubular Joints	2-18
2.3.4	Foundation Bay	2-19
	Ultimate Lateral Strength of Pile Foundations	2-19
	Ultimate Axial Strength of Pile Foundations	2-23
2.3.5	Damaged and Grout-Repaired Members	2-25
	Dents and Global Bending Damage (Loh's Interaction Equations)	2-25
	Corrosion Damage	2-26
	Grout-Repaired Tubular Members (Parsanejad Method)	2-26
2.4	Reliability Analysis	2-33
	Component Reliability	2-33
	Loading Formulation	2-35
	Capacity Formulation: Deck Leg's Shear Capacity	2-36
	Capacity Formulation: Jacket Bays' Shear Capacity	2-37
	Capacity Formulation: Foundation	2-39
2.5	Preliminary Design	2-40
2.6	References	2-41

2.1 Overview of Program Operation

ULSLEA operates under the assumption that a template-type platform can be modeled as a combination of series components (deck, jacket, foundation) which are each made up of parallel elements (deck legs, braces and joints in each jacket bay, imbedded piles). Refer to Figure 2.1.1 for component idealization for a typical platform.

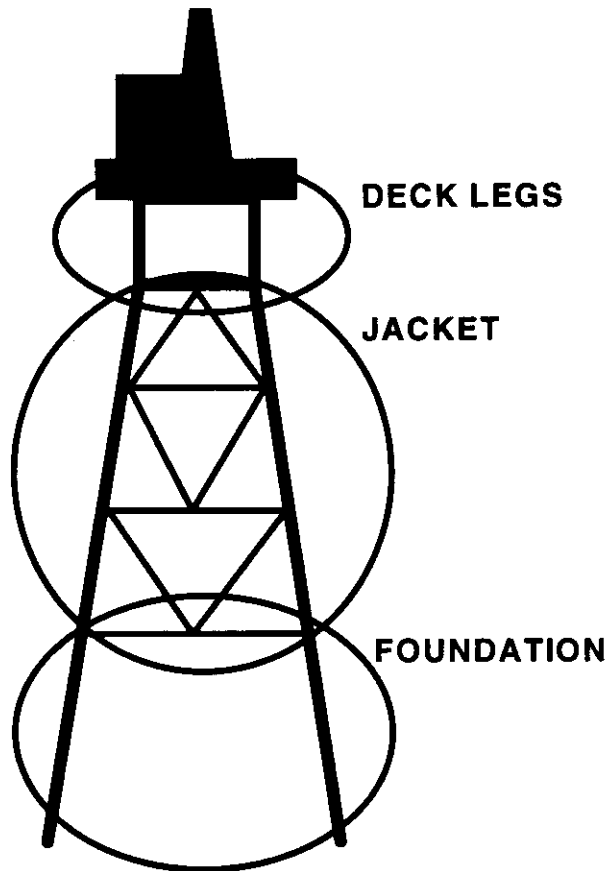


Figure 2.1.1: Primary Structural Components of a Template-Type Platform

The structural strength or capacity of each platform component is formulated based on a presumed failure mode using the principle of virtual work. In order for a component to fail, all of its parallel elements must fail. The component capacities are compared with

the lateral load acting on the component (these loads are due to wind, wave and current acting on the structure); the component whose capacity is exceeded by the applied lateral load is deemed to be the “weak link” in the platform, and hence governs the capacity of the entire structure.

Analyses performed using ULSLEA provide both deterministic results (strength vs. load for each platform component), as well as probabilistic results (β factors) which are calculated based on bias and variability information for elements within the platform and the applied loads supplied by the user.

Figure 2.1.2 illustrates the steps involved in the overall process of the simplified limit equilibrium analysis of an offshore platform. The geometry of the platform is defined by specifying a minimum amount of data. The environmental conditions are defined and include the water depth, wave height and associated period, storm surge depth, current velocity profile and wind speed at a reference elevation. The wind, wave and current are assumed to be acting simultaneously and in the same direction. The wave period is generally taken to be expected period associated with the expected maximum wave height.

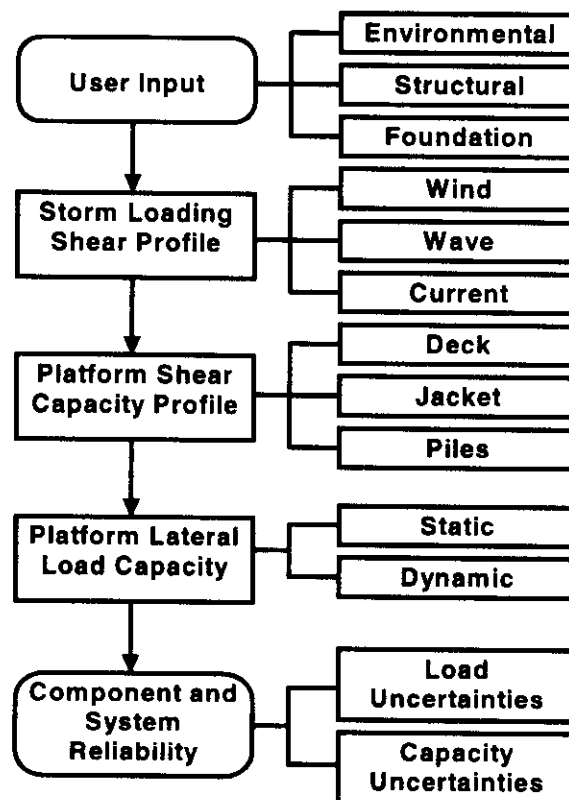


Figure 2.1.2: Simplified Loading, Capacity, and Reliability Analyses Process

The structure is defined by specifying the locations and dimensions of jacket legs, braces, joints, and foundation piles. Specialized elements are designated including grouted or ungrouted joints, braces, and legs. In addition, damaged or defective elements are included. Dent depth and initial out-of-straightness are specified for braces with dents and global bending defects. Element capacity reduction factors may be introduced as biases to account for other types of damage to joints, braces, and foundation (corrosion, fatigue cracks, etc.). Steel elastic modulus, yield strength, and effective buckling length factor (for vertical diagonal braces) are specified. The projected area characteristics of the deck and appurtenances such as boat landings, risers, and well conductors are also specified. If marine fouling is present, the variation of the fouling thickness with depth is defined. Soil characteristics are specified as the depth variation of effective undrained shear strength for cohesive soils or the effective internal angle of friction for cohesionless soils. Scour depth around the piles is also specified.

For the purpose of load calculation, all of the structure elements are modeled as equivalent vertical cylinders that are in line with the wave crest. Appurtenances (boat landings, risers) are modeled in a similar manner. For inclined members, the effective vertical projected area is determined by multiplying the product of member length and diameter by the cube of the cosine of its angle with the horizontal. Wave horizontal velocities are based on Stokes fifth-order theory. The total horizontal water particle velocities are taken as the sum of the wave horizontal velocities and the current velocities. Modification factors are introduced to recognize the effects of wave directional spreading and current blockage. The maximum drag force acting on the portions of structure below the wave crest is based on the fluid velocity pressure. For wave crest elevations that reach the lower decks, the horizontal hydrodynamic forces acting on the lower decks are computed based on the projected area of the portions of the structure that would be able to withstand the high pressures. The wind force acting on the exposed decks is based on the wind velocity pressure.

To develop a resistance profile, collapse mechanisms are assumed for the deck legs, the jacket, and the pile foundation. Based on the presumed failure modes, the principle of virtual work is utilized to estimate the ultimate lateral capacity for each component and a profile of horizontal shear capacity of the platform is developed.

Comparison of the storm shear profile with the platform shear capacity profile identifies the weak-link in the platform system. The base shear or total lateral loading at which the capacity of this weak-link is exceeded defines the static ultimate lateral load capacity of the platform.

The maximum static force acting on and capacities of platform elements and components may be treated as functions of random variables. By taking into account uncertainties associated with loads and capacities and using a First Order Second Moment (FOSM) approach, bounds on probability of system failure are estimated

A typical output of the deterministic failure analysis procedure is illustrated in Figure 2.1.3. Storm shear and platform shear resistance profiles are plotted versus platform elevation. The cumulative storm shear at a given elevation, includes the integrated wind, wave and current forces acting on the portions of platform above that elevation. The storm shear at the top of the plot corresponds to total wind, wave and current forces acting on the deck areas of the platform. The storm shear at the mudline defines the total base shear. The upper-bound capacity of a given bay is based on failure of all of the resisting elements. The lower-bound capacity of a given bay is based on first member failure and is plotted in addition to upper-bound capacity for jacket bays. Comparison of the storm shear and platform capacity profiles identifies the weak-link of the platform. When the lateral load acting on the weakest component equals the shear resistance of this component, the corresponding total base shear defines the ultimate lateral loading capacity of the platform.

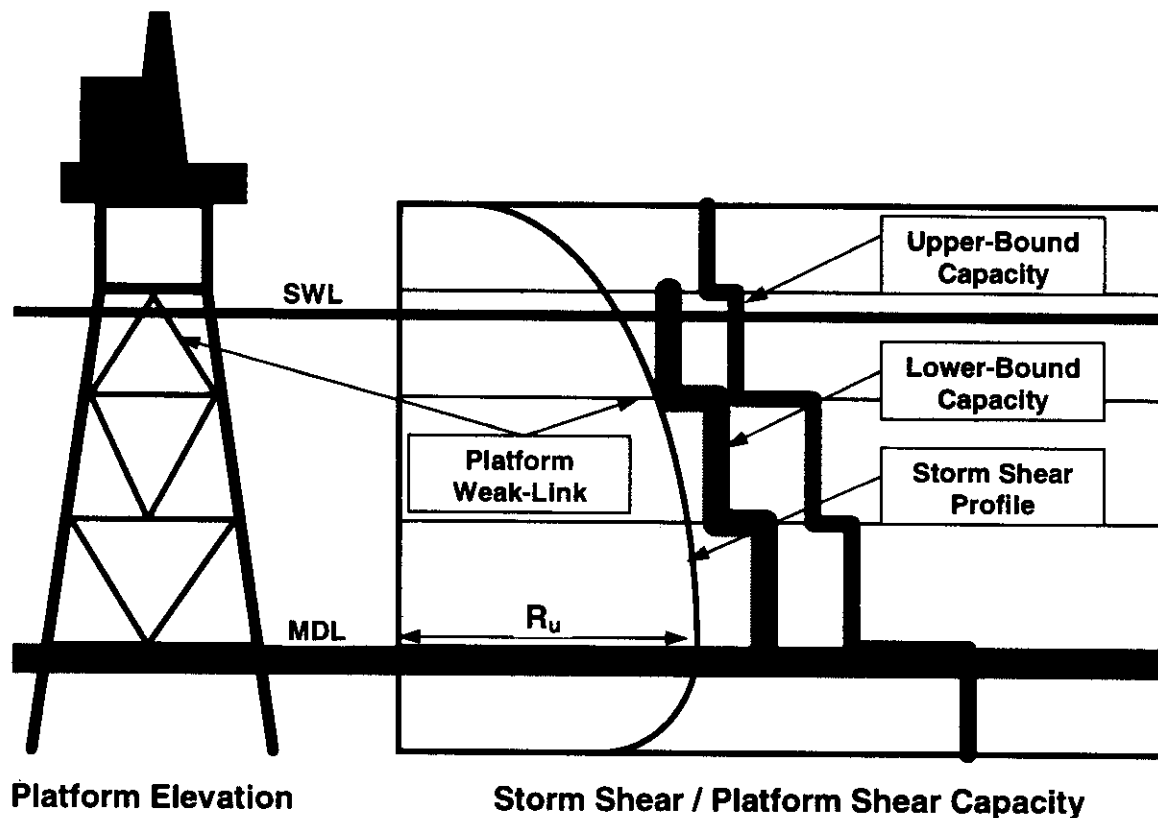


Figure 2.1.3: Typical Output of the Deterministic Failure Analysis

Figure 2.1.4 shows a typical output of the probabilistic failure analysis procedure. The outcome of this procedure is expressed in terms of reliability indices. Reliability index is a measure of safety. For each loading direction, reliability indices, β , are plotted for all failure modes. In addition to the expected values of loadings and capacities, the reliability indices reflect the uncertainties associated with these variables. The probability of failure of each component, p_{fi} , is estimated as $\Phi(-\beta)$, i.e. the normal cumulative distribution function evaluated at $-\beta$. Bounds on the probability of failure of the platform system may be estimated as:

$$\max P_{fi} < P_{fs} < \sum_i P_{fi} \quad (2.1.1)$$

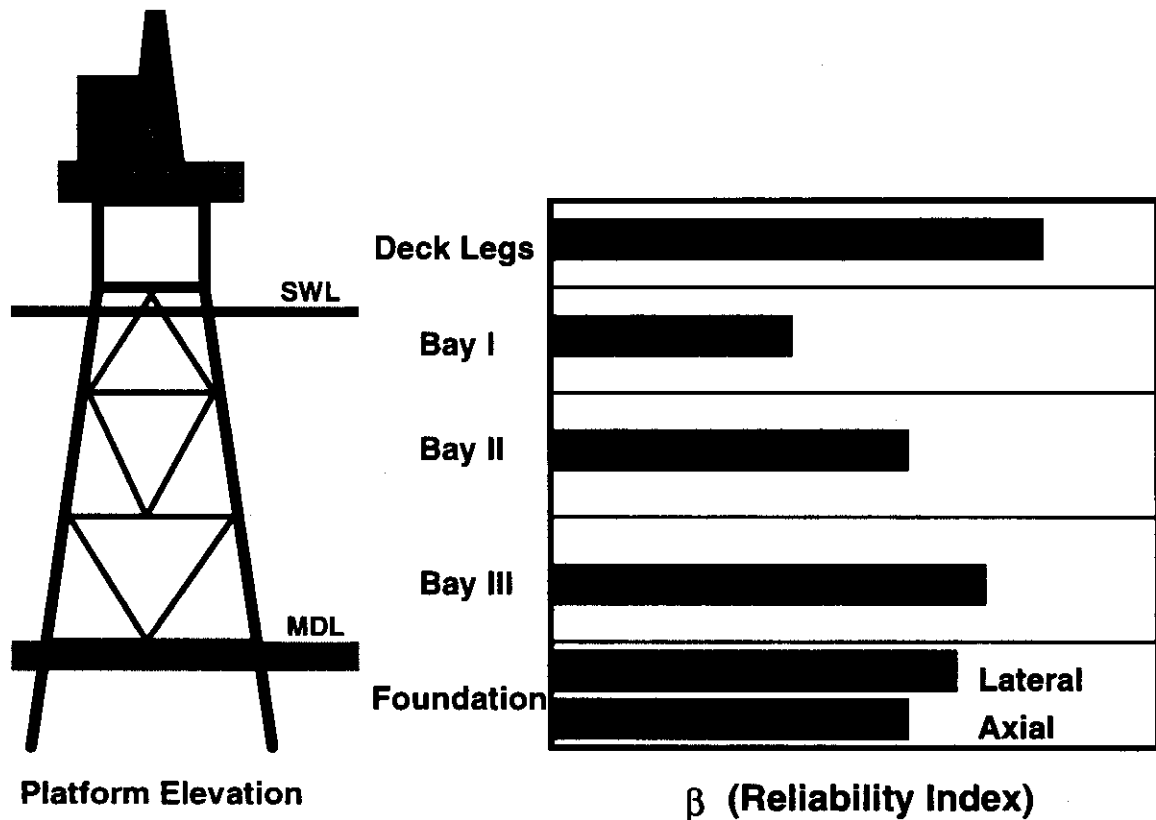


Figure 2.1.4: Typical Output of the Probabilistic Failure Analysis

2.2 Environmental Load Formulation

This section discusses the simplified loading model implemented in ULSLEA to calculate the forces imposed on a platform by wind, wave and currents.

2.2.1 Wind Loads

Given the wind velocity, the maximum wind force, S_a , acting on the exposed decks of the platform is given as:

$$S_a = \frac{\rho_a}{2} C_s A_d V_d^2 \quad (2.2.1.1)$$

where ρ_a is the mass density of air, C_s the wind velocity pressure (or shape) coefficient, A_d the effective projected area of the exposed decks, and V_d the wind velocity at the deck elevation and for an appropriate time interval. The wind shape coefficient is a function of air turbulence, structure geometry and surface roughness.

2.2.2 Wave and Current Loads

Wave horizontal velocities are based on Stokes fifth-order theory. Using equations given by Skjelbreia and Hendrickson (1961) and Fenton (1985), and given the wave height H , period T and water depth d , the vertical profile of maximum horizontal velocities beneath the wave crest is calculated as:

$$u = K_{ds} c \sum_{n=1}^5 n \phi_n' \cosh(nks) \quad (2.2.2.1)$$

where K_{ds} is a coefficient that recognizes the effects of directional spreading and wave irregularity on the Stokes wave theory based velocities. k is the wave number and s is the height above the sea floor. c is the wave celerity and given by:

$$\frac{c^2}{gd} = \frac{\tanh(kd)}{kd} [1 + \lambda^2 C_1 + \lambda^4 C_2] \quad (2.2.2.2)$$

The crest elevation η is estimated by:

$$k\eta = \sum_{n=1}^5 \eta_n \quad (2.2.2.3)$$

ϕ'_n and η'_n are functions of λ and kd . C_n are known functions of kd only and given by Skjelbreia and Hendrickson (1961). The wave number k is obtained by implicitly solving the following equation given by Fenton (1985):

$$\frac{2\pi}{T(gk)^{0.5}} - C_0 - \left(\frac{kH}{2}\right)^2 C_2 - \left(\frac{kH}{2}\right)^4 C_4 = 0 \quad (2.2.2.4)$$

The parameter λ is then calculated using the equation given by Skjelbreia and Hendrickson (1961):

$$\frac{2\pi d}{gT^2} = \frac{d}{L} \tanh(kd) \left[1 + \lambda^2 C_1 + \lambda^4 C_2 \right] \quad (2.2.2.5)$$

Having the parameters λ and kd , Equations (2.2.2.1) and (2.2.2.3) can be used to estimate the horizontal water particle velocities and the wave crest elevation. The specified variation of current velocities with depth is stretched to the wave crest and modified to recognize the effects of structure blockage on the currents. The total horizontal water particle velocities are taken as the sum of the wave horizontal velocities and the current velocities.

The maximum drag force acting on the portions of structure below the wave crest is based on the fluid velocity pressure component of the Morison equation:

$$F_d = \frac{1}{2} C_d \rho A u |u| \quad (2.2.2.6)$$

where ρ is the mass density of water, A the effective vertical projected area of the exposed structure element, and u the horizontal velocity of water at a given point on the submerged portion of the structure element. Due to 90 degree phase angle difference between the maximum drag and inertia force components and the relatively small dimensions of a typical jacket-type platform with respect to wave lengths and heights in an extreme condition, at the time the drag forces acting on the platform reach a maximum value the inertia forces are relatively small; hence, only the drag force component of Morison equation is estimated.

All of the structure elements are modeled as equivalent vertical cylinders that are in line with the wave crest (Figure 2.2.2.1). Appurtenances (boat landings, risers) are modeled in a similar manner. For inclined members, the effective vertical projected area is determined by multiplying the product of member length and diameter by the cosine of its angle with the horizontal.

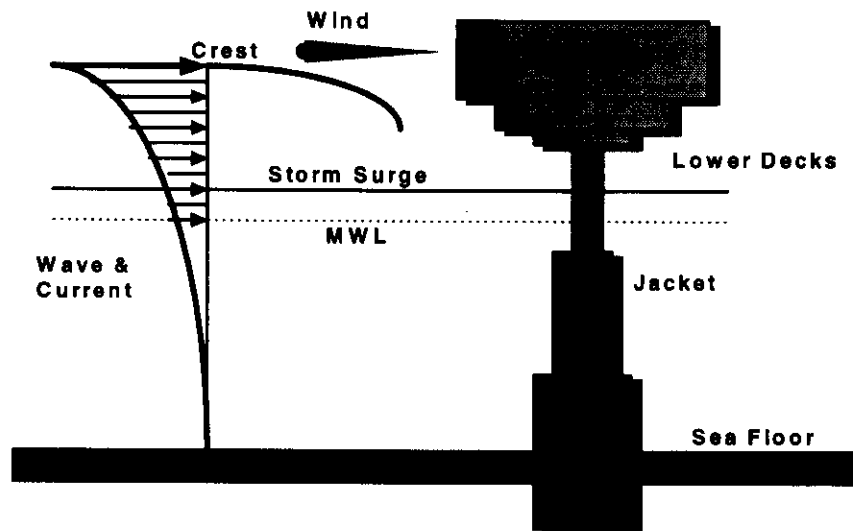


Figure 2.2.2.1: Simplified Load Model

For wave crest elevations that reach the lower decks, the horizontal hydrodynamic forces acting on the lower decks are computed based on the projected area of the portions of the structure that would be able to withstand the high pressures. The fluid velocities and pressures are calculated in the same manner as for the other submerged portions of the structure. C_d , defined by the user for both decks and members, is assumed to be developed at a depth equal to two velocity heads (U^2/g) below the wave crest. In recognition of the near wave surface flow distortion effects, C_d is assumed to vary linearly from its value at two velocity heads below the wave crest to zero at the wave crest. (McDonald et al., 1990; Bea and DesRoches, 1993).

2.3 Ultimate Strength Formulations for Platform Components

Using the concept of plastic hinge theory, limit equilibrium for each platform component is formulated by implementing the principle of virtual work. This is the key to the simplified ultimate limit state analysis method. Where of importance, geometric and material nonlinearities are considered. This method is being increasingly used in plastic design of simple structures or structural elements (e.g. moment frames, continuous beams). Due to the impracticality of such analyses for more complicated structures, these methods have not found broad use in design or assessment of complex structures; all possible failure modes need to be considered and evaluated to capture the “true” collapse mechanism and the associated ultimate lateral load.

Actual field experience and numerical results from three-dimensional, nonlinear analyses performed on a variety of template-type platforms indicate that in most cases certain failure modes govern the ultimate capacity of such platforms: a) plastic hinge formation in the deck legs and subsequent collapse of the deck portal, b) buckling of the main load carrying vertical diagonal braces in the jacket, c) lateral failure of the foundation piles due to plastic hinge formation in the piles and plastification of foundation soil, and d) pile pullout or pile plunging due to exceedance of axial pile and soil capacities.

Based on experience, collapse mechanisms are assumed for the three primary components that comprise a template-type platform: the deck legs, the jacket, and the pile foundation. Based on the presumed failure modes, the principle of virtual work is utilized to estimate the ultimate lateral capacity for each component. This process is described in detail for the primary components of a platform in the following subsections.

2.3.1 Deck Bay

The ultimate shear that can be resisted by an unbraced deck portal is estimated based on bending moment capacities of the tubular deck legs that support the upper decks. A collapse mechanism in the deck bay would form by plastic yielding of the leg sections at the top and bottom of all of the deck legs (Figure 2.3.1.1). The interaction of bending moment and axial force is taken into account. The maximum bending moment and axial force that can be developed in a tubular deck leg is limited by local buckling of leg cross-sections. The vertical dead loads of the decks are assumed to be equally shared among the deck legs. Due to relatively large axial loads (weight of the decks and topside facilities) and large relative displacements at collapse (deck bay drift), P - Δ effect plays a role in reducing the lateral shear capacity and hence is taken into account.

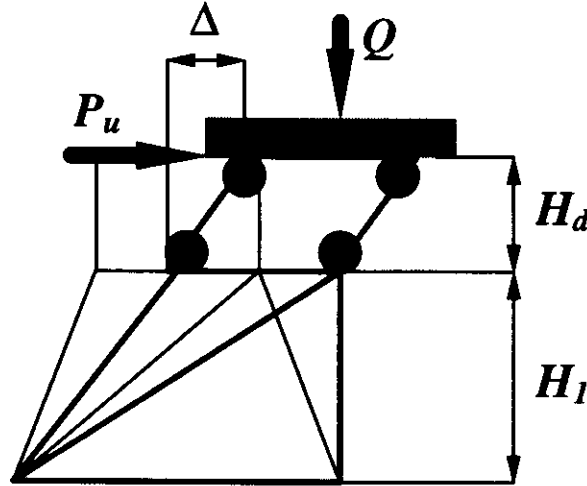


Figure 2.3.1.1 : Deck Portal at Ultimate Lateral Load

Deck Bay Drift at Collapse:

To derive an estimate of $P-\Delta$ effect with out leaving the framework of a simplified analysis, simplifying assumptions are made. It is assumed that the deck structure is rigid. It is further assumed that plastic yielding of the sections at the bottom of the deck legs occur simultaneously, following the plastic yielding of the sections at the top of the legs and hence an estimate of plastic hinge rotations to calculate the deck bay drift is unnecessary. Finally, to estimate the deck bay drift at collapse, Δ , the jacket is replaced by rotational springs at the bottom of each deck leg. The spring rotational stiffness, C_r , is approximated by applying external moments, which are equal in magnitude and have the same direction, to the top of jacket legs at the uppermost jacket bay. Assuming rigid horizontal braces and fixed boundary conditions at the bottom of these jacket legs, the rotation of cross-sections at the top of the legs and hence the rotational stiffness, C_r , is determined:

$$\frac{1}{C_r} = \frac{H_l}{E I_l \cos \beta} \left(1 - \frac{3 C_s H_l^3}{4 C_s H_l^3 + 12 E I_l \cos \beta} \right) \quad (2.3.1.1)$$

where C_s is an equivalent lateral stiffness coefficient:

$$C_s = \frac{1}{2} \sum_i \frac{\cos^2 \theta_i E_i A_i}{L_i} \quad (2.3.1.2)$$

summed over all diagonal braces within the uppermost jacket bay. I_l and H_l denote the moment of inertia of the jacket leg and the first jacket bay height respectively. E is the

Young modulus, β and θ are the batter angle of the jacket legs and vertical diagonal braces respectively.

The principle of virtual force is implemented to calculate the deck bay horizontal drift at collapse:

$$\Delta = M_u H_d \left(\frac{H_d}{6 E I_d} + \frac{1}{C_r} \right) \quad (2.3.1.3)$$

H_d and I_d are the height and moment of inertia of the deck legs. M_u is the ultimate moment that can be resisted by the cross-section in the presence of axial load and can be derived from the M - P interaction equation for tubular cross-sections:

$$M_u = M_{cr} \cos \left(\frac{\pi}{2} \frac{Q / n}{P_{cr}} \right) \quad (2.3.1.4)$$

M_{cr} and P_{cr} denote the critical moment and axial load associated with local buckling of the tubular cross-section. Q denotes the total vertical deck load and n is the number of supporting deck legs.

Deck Legs Lateral Shear Strength:

Using the formulation developed above for the deck bay drift at collapse, the lateral shear capacity of the deck portal can be estimated. Equilibrium is formulated using the principle of virtual displacement. Using the actual collapse mechanism as the virtually imposed displacement, the equilibrium equation for the lateral shear capacity of the unbraced deck portal is derived including the second-order P - Δ effect:

$$P_u = \frac{I}{H_d} (2n M_u - Q\Delta) \quad (2.3.1.5)$$

2.3.2 Jacket Bays

The shear capacity of each of the bays of vertical bracing that comprise the jacket is estimated including the tensile and compressive capacity of the diagonal braces and the associated joint capacities. The capacity of a given brace is taken as the minimum of the capacity of the brace or the capacity of either its joints. The batter component of axial force in the jacket legs and piles inside the jacket legs are taken into account. Where of significance, the shear forces in the legs and piles are also considered.

Ultimate Axial Strength of Tubular Braces:

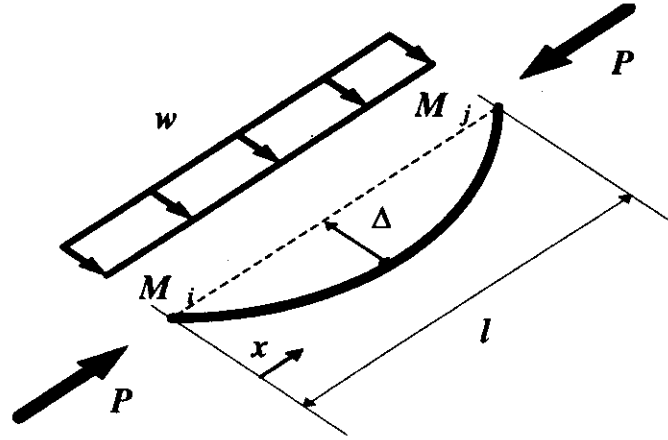


Figure 2.3.2.1: Brace Element Under Compressive and Transverse Loading

The diagonal braces near the free surface are exposed to high combined bending moments and axial forces. In general, the existing bending moment result in a reduction of the ultimate axial load capacity of the brace. At the ultimate state, the large deflections result in inelastic strains. Generally an elastic-plastic load deflection (P - δ) analysis should be performed to determine the ultimate strength of the brace. The braces are treated as though there are no net hydrostatic pressures (e.g. flooded members). The governing differential equation of the beam-column can be given as:

$$M_{xx} + \frac{P}{EI} M = -w - 8P \frac{\Delta_0}{l^2} \quad (2.3.2.1)$$

where M_{xx} stands for the second derivative of bending moment with regard to the coordinate x (Figure 2.3.2.1). Δ_0 , P , and l are the initial out-of-straightness, axial force and unbraced length of the member respectively. The following substitutions:

$$\xi = \frac{x}{l}, \quad \epsilon = l \sqrt{\frac{P}{EI}} \quad (2.3.2.2), (2.3.2.3)$$

result in the transformed differential equation:

$$M_{\xi\xi} + \epsilon^2 M = -w l^2 - 8P \Delta_0 \quad (2.3.2.4)$$

This equation has the following closed-form solution:

$$M(\xi) = \frac{\sin \epsilon (1 - \xi)}{\sin \epsilon} M(\xi = 0) + \frac{\sin \epsilon \xi}{\sin \epsilon} M(\xi = 1) + \frac{1}{\epsilon^2} \left(\frac{\cos \epsilon (0.5 - \xi)}{\cos \frac{\epsilon}{2}} - 1 \right) (w l^2 + 8 P \Delta_0) \quad (2.3.2.5)$$

Based on a three-hinge failure mode, the exact solution of the second-order differential equation for the bending moment of a beam-column (Equation 2.3.2.5) is implemented to formulate the equilibrium at collapse:

$$M(\xi = 0.5) = -M(\xi = 0) = -M(\xi = 1) = M_u \quad (2.3.2.6)$$

$$M_u = \left(\frac{1}{1 + 2 \frac{\sin 0.5 \epsilon}{\sin \epsilon}} \right) \frac{1}{\epsilon^2} \left(\frac{1}{\cos \frac{\epsilon}{2}} - 1 \right) (w l^2 + 8 P_u \Delta_0) \quad (2.3.2.7)$$

Elastic-perfectly plastic material behavior is assumed. The ultimate compression capacity is reached when full plastification of the cross-sections at the member ends and mid-span occur (Figure 2.3.2.2). It is further assumed that plastic hinges at member ends form first followed by plastic hinge formation at mid-span. M - P interaction condition for tubular cross-sections provides a second equation for the unknown ultimate moment M_u and axial force P_u in plastic hinges at collapse:

$$\frac{M_u}{M_p} - \cos \left(\frac{\pi}{2} \frac{P_u}{P_p} \right) = 0 \quad (2.3.2.8)$$

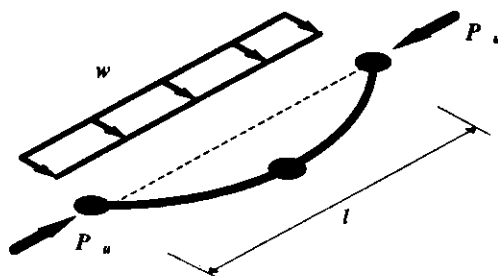


Figure 2.3.2.2: Three Hinge Failure Mode for Diagonal Braces

The results of this formulation have been verified with results from the nonlinear finite element program USFOS (Sintef, 1994); using the same initial out-of-straightness, Δ_0 , for both simplified and complex analyses, the axial compression capacity of several critical diagonal members of different structures has been estimated. The simplified method slightly overpredicts the axial capacity of compression members (less than 10%). The initial out-of-straightness, Δ_0 , is used to calibrate the axial compression capacity of braces to the column buckling curves according to API RP 2A-LRFD (API, 1993):

$$\Delta_0 = \frac{M_p \cos\left(\frac{\pi}{2} \frac{P_{cr}}{P_p}\right)}{\left(\frac{1}{1+2 \frac{\sin 0.5\epsilon}{\sin \epsilon}}\right) \frac{1}{\epsilon^2} \left(\frac{1}{\cos \frac{\epsilon}{2}} - 1\right) (8 P_{cr})} \quad (2.3.2.9)$$

where P_{cr} is the buckling load of a given brace according to API RP 2A-LRFD. Using appropriate buckling effective length factors (0.65 is recommended as realistic), the calibrated results are in close agreement with results from USFOS (Hellan et al., 1994).

Effect of Shear Force in Jacket Legs and Piles:

Within the framework of a simplified analysis, the jacket has been treated as a trusswork. Plastic hinge formation in the jacket legs was not considered because this hinge development occurs at a lateral deformation that is much larger than is required to mobilize the axial capacities of the vertical diagonal braces. At the large lateral deformations required to mobilize the lateral shear capacities of the legs, the diagonal brace capacities have decreased significantly due to column buckling or tensile rupture. In general, the effect of bending moment distribution along the jacket legs on the lateral capacity has been neglected. This assumption is justified by the following example.

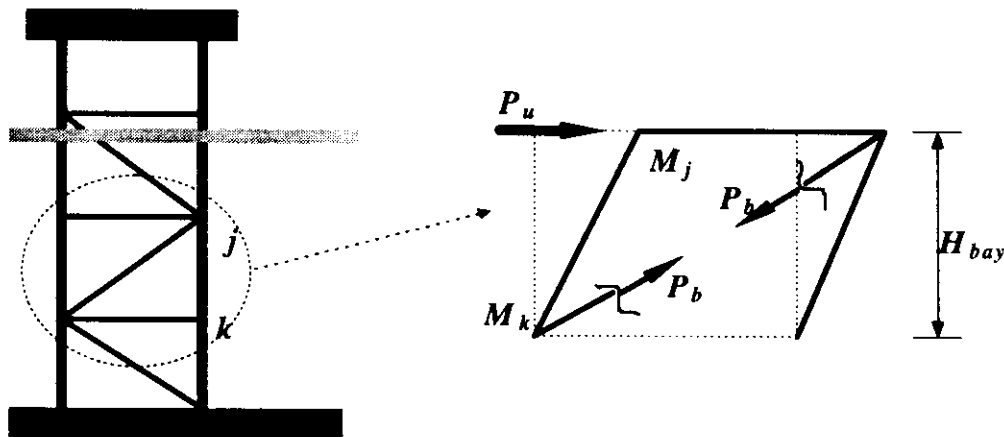


Figure 2.3.2.3 : Lateral Capacity of a Jacket Bay

A virtual displacement is imposed to the i^{th} jacket bay of a two-dimensional jacket frame (Figure 2.3.2.3), and the external and internal work equated:

$$W^{(E)} = W^{(I)} \quad (2.3.2.14)$$

which leads to the following equilibrium equation for the given jacket bay:

$$P_u = P_{bh} + \frac{2(M_j + M_k)}{H_{bay}} \quad (2.3.2.15)$$

where P_{bh} denotes the horizontal component of brace axial force. Assuming that the magnitude of bending moment in the jacket legs is negligible:

$$M_j = M_k = 0 \quad (2.3.2.16)$$

the following simplified relationship results:

$$P_u = P_{bh} \quad (2.3.2.17)$$

This assumption leads to estimates of lateral capacity of a jacket bay that are either conservative or unconservative depending on the actual bending moment distribution in the legs. However, this conservatism or unconservatism is negligible for all but the uppermost and lowest jacket bays. Due to frame action in the deck portal and rotational restraint of the legs at mud level, the jacket legs and piles inside the legs experience relatively large bending moments at these two bays. The bending moment in the legs at the lowest bay has the direction of a resisting moment and hence not considering it can only be conservative. However, the shear force due to the large moment gradient at the uppermost jacket bay has the same direction as the global lateral loading. If this effect is not taken into account, the lateral capacity will be overestimated.

A simplified procedure is developed to account for the effect of shear force in the top jacket bay. Of interest is the moment distribution along the legs at this bay due to frame action in the deck portal (Figure 2.3.2.4). Given the geometry of the deck portal and the load acting on deck areas, the moment distribution along the deck legs can be estimated:

$$M_o = \frac{\frac{P_d L_d^2}{2EI} + \frac{P_d L_d}{C_r}}{\frac{L_d}{EI} + \frac{1}{C_r}} \leq M_p \quad (2.3.2.17)$$

$$M_j = M_o - P_d L_d \leq M_p \quad (2.3.2.18)$$

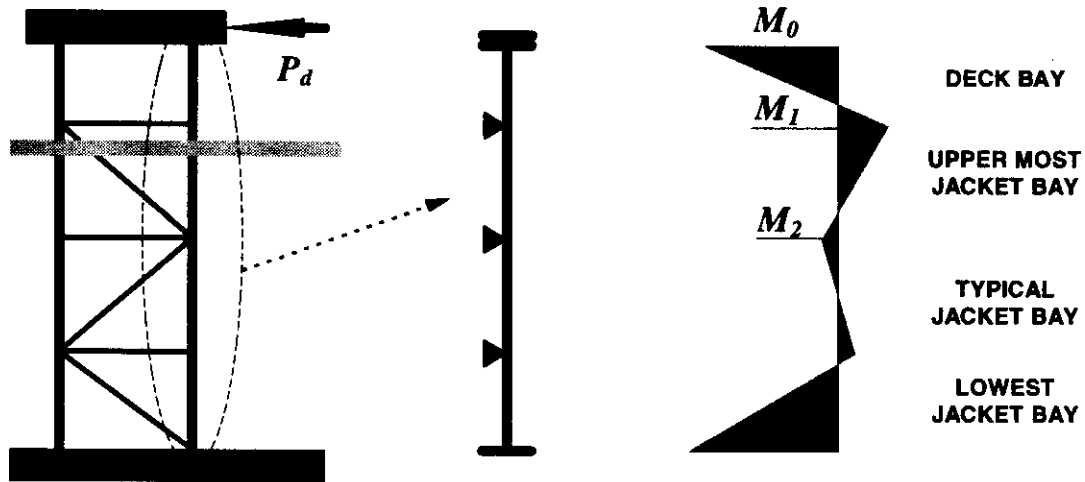


Figure 2.3.2.4 : Moment Distribution in Jacket Legs under Lateral Loading

Thinking of a jacket leg as a continuous beam which is supported by horizontal framings, the applied moment at the top of the leg rapidly decreases towards the bottom. Based on geometry of the structure, in particular jacket bay heights and the cross-sectional properties of the jacket leg (if nonprismatic), and in the limiting case of rigid supports, an upper bound for the desired moment distribution is estimated. For equal spans, constant moment of inertia and limiting case of rigid supports the following relationship can be derived:

$$|M_2| \leq 0.286 |M_1| \quad (2.3.2.19)$$

This relationship is then used together with Equation (2.3.2.15) to estimate the capacity of the jacket bay.

Jacket Bays Lateral Shear Strength:

To derive a lower-bound capacity formulation, the notion of Most Likely To Fail (MLTF) element is introduced. MLTF element is defined as the member with the lowest capacity over stiffness ratio. The lower-bound lateral capacity of a jacket bay is estimated by adding the horizontal force components of all load carrying members in the given bay at the instant of first member failure. A linear multi-spring model is used to relate the forces and displacements of diagonal braces within a bay. It is assumed that the horizontal braces are rigid. The axial force in the jacket legs due to lateral overturning moment is estimated at each bay and its batter component is added to the lateral capacity:

$$P_{u,l} = \sum_i \left(\frac{P_{u,MLTF}}{K_{MLTF}} \right) K_i + F_L \quad (2.3.2.20)$$

The summation is over all vertical diagonal braces within a given jacket bay. $P_{u,l}$ denotes the lower-bound lateral shear capacity of the jacket bay, P_u is the horizontal component of axial force in a given diagonal brace, F_L is the sum of batter components of leg forces, and K_i denotes the lateral stiffness of brace i :

$$K_i = \frac{E_i A_i \cos^2 \theta}{L_i} \quad (2.3.2.21)$$

where L , E , A , and θ denote the length, Young modulus, cross-sectional area, and the angle between the diagonal brace and the horizon respectively.

An upper-bound capacity is also formulated for each bay. After the MLTF member in compression reaches its axial capacity, it cannot maintain the peak load and any further increase in lateral displacement will result in unloading of this member. Presuming that the load path remains intact (inter-connecting horizontals do not fail), a load redistribution follows and other members carry the load of the lost members until the last brace reaches its peak capacity. An empirical residual capacity modification factor, α , is introduced. Assuming elasto-perfectly plastic material behavior, α is equal to 1.0 for members in tension (neglecting strain hardening effects) and less than 1.0 for members in compression due to P - δ effects (generally in the range of 0.15 to 0.5). The upper-bound lateral shear capacity of a given jacket bay, $P_{u,u}$, is estimated by adding the horizontal component of the residual strength of all of the braces within the bay:

$$P_{u,u} = \sum_i P_{ui} \alpha_i + F_L \quad (2.3.2.22)$$

2.3.3 Ultimate Strength of Tubular Joints

Experience has shown that tubular connections have a high plastic reserve strength beyond first yield, which can not be addressed by conventional linear elastic methods. Hence, empirical capacity equations based on test results have been used to predict the joint ultimate strength. Based on a data base of 137 tests of tubular joints, Yura et al. (1980) recommended one formula for both compressive and tensile ultimate capacity in the branch of a K-joint. This formula is identical to that for T and Y joints except for the additional gap factor. The test capacity was taken as the lowest of the loads at first crack, at an excessive deformation, or at first yield. For simple tubular joints with no gussets, diaphragms, or stiffeners, the capacity equations are given in Table 2.3.3.1. The same capacity equations are adopted by API RP 2A-LRFD (API, 1993).

Joint Type	Tension	Compression
T, Y	$\frac{f, T^2 (3.4 + 19\beta)}{\sin \Theta}$	$\frac{f, T^2 (3.4 + 19\beta)}{\sin \Theta}$
DT, X	$\frac{f, T^2 (3.4 + 19\beta)}{\sin \Theta}$	$\frac{f, T^2 (3.4 + 19\beta)}{\sin \Theta} Q_\beta$
K	$\frac{f, T^2 (3.4 + 19\beta)}{\sin \Theta} Q_\gamma$	$\frac{f, T^2 (3.4 + 19\beta)}{\sin \Theta} Q_\gamma$

Table 2.3.3.1: Capacity Equations for Simple Tubular Joints (Yura et al., 1980)

Q_β is a factor accounting for geometry and Q_γ is a gap modifying factor and are estimated according to the following equations:

$$Q_\gamma = 1.8 - 0.1 \frac{g}{T} \quad \text{for} \quad \gamma \leq 20 \quad (2.3.3.1)$$

$$Q_\gamma = 1.8 - 4 \frac{g}{D} \quad \text{for} \quad \gamma > 20 \quad (2.3.3.2)$$

$$Q_\beta = \frac{0.3}{\beta(1 - 0.833\beta)} \quad \text{for} \quad \beta > 0.6 \quad (2.3.3.3)$$

$$Q_\beta = 1.0 \quad \text{for} \quad \beta \leq 0.6 \quad (2.3.3.4)$$

g denotes the gap between branches of K-joints, $\beta = d/D$, and $\gamma = d/2T$. D , d and T are the branch and chord diameter and thickness respectively.

The capacity equations given above are known to be conservative (API, 1993). Bias factors may be input by the user to increase the effective capacity if desired.

2.3.4 Foundation Bay

Two measures of strength are used for the foundation bay: lateral and axial.

Ultimate Lateral Strength of Pile Foundations:

The pile lateral shear capacity is based on an analysis similar to that of deck legs with the exception that the lateral support provided by the foundation soils and the batter shear component of the piles are included. It is assumed that each pile reaches its ultimate lateral capacity when two plastic hinges form: one at the mudline and the other at a lower depth where the bending moment reaches a maximum (Figure 2.3.4.1). Figure 2.3.4.2 shows the assumed lateral pile failure mode in cohesive soils.

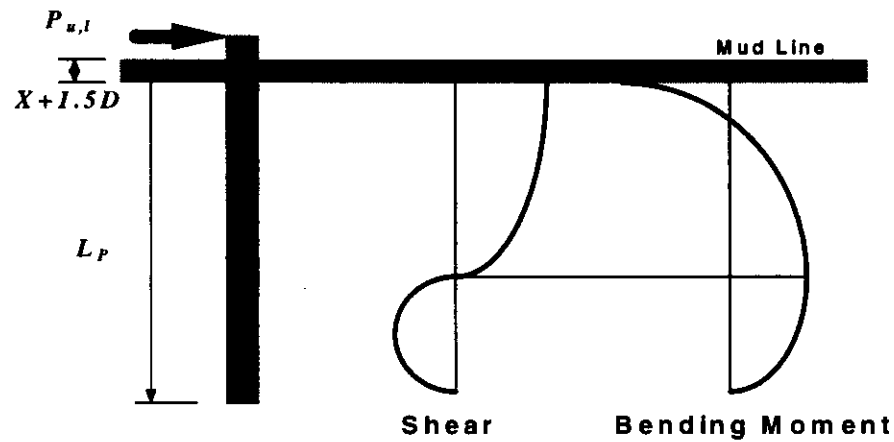


Figure 2.3.4.1 : Internal Force Distribution in a Vertical Laterally Loaded Pile

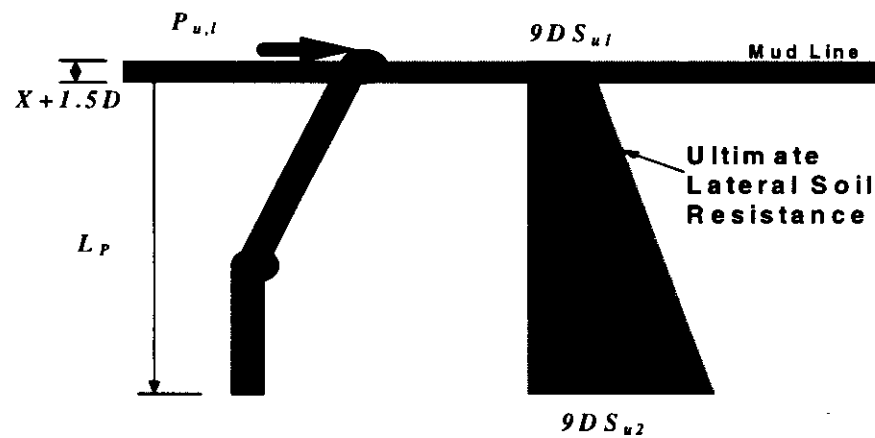


Figure 2.3.4.2 : Lateral Pile Failure Mode in Cohesive Soil

For cohesive soils, the distribution of lateral soil resistance along the pile per unit length, p_s , is assumed to be:

$$p_s = 9 S_u D \quad (2.3.4.1)$$

where S_u is the effective undrained shear strength of the soil and D is the pile diameter. This formulation, which is used in ULSLEA, is supported by studies of Matlock (1970) and Randolph et al. (1984) for smooth piles. Findings by Reese et al. (1975) support a lateral soil resistance of $11S_uD$.

Based on Equation (2.3.4.1) and for a constant undrained shear strength, S_u , over the pile length and for a given scour depth, X , the ultimate lateral force that can be developed at the pile top is (Tang, 1990):

$$P_{u,l} = 0.5 \left\{ - \left(27 D^2 S_u + 18 S_u X D \right) + \left[\left(27 D^2 S_u + 18 S_u X D \right)^2 + 144 S_u D M_u \right]^{0.5} \right\} \quad (2.3.4.2)$$

where M_u is the plastic moment capacity of the pile cross-section computed using the M - P interaction equation for tubular cross sections. In the case of linearly increasing shear strength with depth the ultimate lateral capacity of the pile, $P_{u,l}$, can be estimated from the following equation:

$$P_{u,l} \left(C + \xi \right) - 2 M_u - \left(A + \eta \xi \right) \frac{C^2}{2} - \left(\frac{\eta}{2} \right) \frac{C^3}{3} = 0 \quad (2.3.4.3)$$

where:

$$C = \frac{1}{\eta} \left[\left(-A + \eta \xi \right) + \sqrt{\left(A + \eta \xi \right)^2 + 2 \eta P_{u,l}} \right] \quad (2.3.4.4)$$

$$\eta = \frac{B - A}{L_p} \quad (2.3.4.5)$$

$$\xi = 15D + X \quad (2.3.4.6)$$

$$A = 9 S_{u1} D \text{ and } B = 9 S_{u2} D \quad (2.3.4.7), (2.3.4.8)$$

S_{u1} and S_{u2} denote the undrained shear strength at mudline and at the pile tip respectively (Figure 2.3.4.2). For cohesionless soils, the distribution of lateral soil pressure along a pile at a depth z , is assumed to be:

$$p_s = 3 \gamma z K_p \quad (2.3.4.9)$$

where:

$$K_p = \tan^2 \left(45 + \frac{\Phi}{2} \right) \quad (2.3.4.10)$$

Φ is the effective angle of internal friction of the soil and γ is the submerged unit weight of the soil. The ultimate lateral force that can be developed at the pile top with no scour is (Tang, 1990):

$$P_{u,l} = 2.382 M_p^{2/3} (\gamma D K_p)^{1/3} \quad (2.3.4.11)$$

For a scour depth equal to X , the ultimate lateral force is given implicitly by:

$$P_{u,l} = \frac{2 M_p}{\left[X + 0.544 \left(\frac{P_{u,l}}{\gamma D K_p} \right) \right]^{0.5}} \quad (2.3.4.12)$$

The equilibrium equations (2.3.4.2), (2.3.4.3), (2.3.4.11) and (2.3.4.12) are derived using the principle of virtual displacement. The horizontal batter component of the pile top axial force is added to estimate the total lateral shear capacity of the piles. This component is computed based on axial loads carried by the piles due to storm force overturning moment.

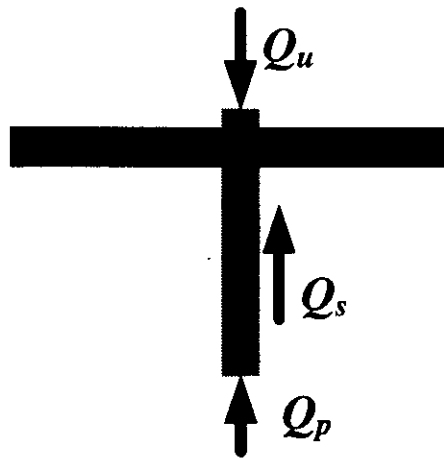


Figure 2.3.4.3: Axial Pile Capacity

Ultimate Axial Strength of Pile Foundations:

The axial resistance of a pile is based on the combined effects of a shear yield force acting on the lateral surface of the pile and a normal yield force acting over the entire base end of the pile (Figure 2.3.4.3). Thus the ultimate axial capacity Q_u , can be expressed as:

$$Q_u = Q_s + Q_p = q A_p + f_{av} A_{sh} \quad (2.3.4.13)$$

Q_p denotes the ultimate end bearing and Q_s is the ultimate shaft capacity, q is the normal end yield force per unit of pile-end area acting on the area of pile tip A_p , and f_{av} denotes the ultimate average shear yield force per unit of lateral surface area of the pile acting on embedded area of pile shaft A_{sh} . It is assumed that the pile is rigid and that shaft friction and end bearing forces are activated simultaneously. It is further assumed that the spacing of the piles is sufficiently large so that there is no interaction between the piles.

After considering the weight of the pile and the soil plug (for open-end piles), the ultimate compressive loading capacity of the pile, Q_c , can be calculated as:

$$Q_c = \frac{q\pi D_o^2}{4} + (f_{av} \pi D_o - w_p) L_p \quad (2.3.4.14)$$

$$w_p = \gamma_{st} A_{st} + \gamma_s A_s = \frac{l}{4} [\gamma_{st} \pi (D_o^2 - D_i^2) + \gamma_s \pi D_i^2] \quad (2.3.4.15)$$

where:

- A_{st} = cross-sectional area of the steel pile
- A_s = cross-sectional area of the soil plug
- D_o = outside diameter of the pile
- D_i = inside diameter of the pile
- f_y = yield stress
- γ_{st} = submerged specific weight of steel
- γ_s = submerged specific weight of soil
- L_p = pile embedded length
- w_p = weight of pile and soil plug per unit length

The end bearing capacity can be fully activated only when the shaft frictional capacity of the internal soil plug exceeds the full end bearing (Focht and Kraft, 1986). This condition can be formulated as:

$$\frac{q\pi D_i^2}{4} < (f_{av} \pi D_i + w_s) L_p \quad (2.3.4.16)$$

The tensile capacity is similarly estimated as:

$$Q_t = (f_{av} \pi D_o + w_p) L_p \quad (2.3.4.17)$$

For cohesive soils with an undrained shear strength, S_u , the ultimate bearing capacity is taken as the end bearing of a pile in clay:

$$q = 9 S_u \quad (2.3.4.18)$$

The ultimate shaft friction is taken as:

$$f_{av} = \kappa S_{u,av} \quad (2.3.4.19)$$

where κ is the side resistance factor and a function of the average undrained shear strength $S_{u,av}$ as given in Table 2.3.4.1. For cohesionless soils, the ultimate bearing capacity of a deeply embedded pile is estimated as:

$$q = N_q \sigma_v \quad (2.3.4.20)$$

N_q is a bearing capacity factor and a function of the friction angle of the soil Φ , and σ_v denotes the effective pressure at the pile tip. Since sand soils possess high permeability, the pore water quickly flows out of the soil mass and the effective stress is assumed equal to applied stress. The unit shaft resistance on pile increment is estimated as:

$$f_i = k \sigma_{vi} \tan \delta \quad (2.3.4.21)$$

where k is an earth lateral pressure coefficient assumed to be 0.8 for both tension and compression loads, σ_{vi} denotes the effective overburden pressure at the given depth, and δ denotes the friction angle between the soil and pile material and is taken as:

$$\delta = \Phi - 5^\circ \quad (2.3.4.22)$$

The unit shaft resistance and the unit end bearing capacity can not indefinitely increase with the penetration. The ultimate axial capacity of piles in sand soils is estimated based on commonly used limiting values for N_q , q_{max} and f_{max} given by Focht and Kraft (1986), (Table 2.3.4.2).

Undrained Shear Strength $S_{u,av}$ (ksf)	Side Resistance Factor κ
<0.5	1
0.5 - 1.5	1 - 0.5
>1.5	0.5

Table 2.3.4.1: Side Resistance Factor for Cohesive Soils (Focht et al., 1986)

Friction Angle Φ	Bearing Cap. Factor, N_q	Bearing Cap. q_{max} (ksf)	Shaft Friction f_{max} (ksf)
20	8	40	1.0
25	12	60	1.4
30	20	100	1.7
35	40	200	2.0

Table 2.3.4.2: Frequently Used Values for Medium Dense Materials (Focht et al., 1986)

2.3.5 Damaged and Grout-Repaired Members

This section addresses the formulations used in evaluating the strengths of damaged and grout-repaired members.

Dents and Global Bending Damage (Loh's Interaction Equations):

Developed at Exxon Production Research Company, BCDENT is a general computer program that uses M - P - Φ approach to evaluate the full behavior of dented member (Loh, 1993). The behavior of the dent section is treated phenomenologically using a set of M - P - Φ expressions. Compared with the experimental results, BCDENT gives mean strength predictions for both dented and undented members. Based on BCDENT results, Loh (1993) presented a set of new unity check equations for evaluating the residual strength of dented tubular members. The unity check equations have been calibrated to the lower bound of all existing test data. The equations cover axial compression and tension loading, in combination with multi-directional bending with respect to dent orientation. When the dent depth approaches zero, the recommended equations are identical to API RP 2A equation for undamaged members (API, 1993). Loh's equations for dent damaged members and those with global bending damage have been integrated in ULSLEA. These equations are listed on pages 27-29.

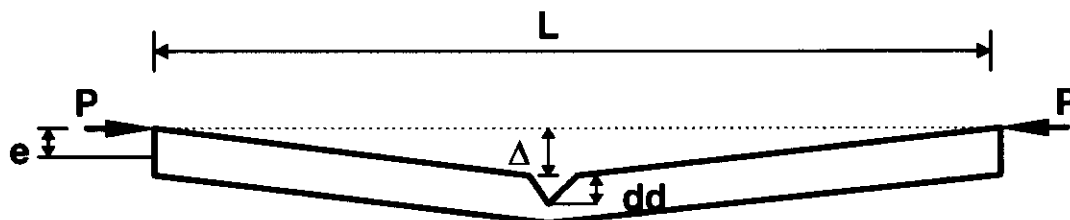


Figure 2.3.5.1: Definition Sketch for a Damaged Tubular Brace

Corrosion Damage:

The marine environment is extremely corrosive. Although cathodic protection systems and protective coatings have been applied to prevent corrosion of steel members, in numerous cases corrosion damage of offshore platforms has still been observed. Corrosion results in a reduced wall thickness of the steel members which can lead to premature local buckling at the corroded areas. ULSLEA incorporates an option to include bias factors, by which a member's strength may be reduced as desired, should there be corrosion damage.

Grout-Repaired Tubular Members (Parsanejad Method):

Responding to the need for some sort of analytical expressions, Parsanejad (1987) presented a simple analytical expression for estimating the ultimate capacity of grout-filled damaged tubular members. The analysis was based on the following simplifying assumptions:

- a) full interaction exists between grout and the damaged tube and
- b) grout provides sufficient support to the tube wall in the damaged region to prevent premature local buckling.

The first yield collapse criterion was adopted by Parsanejad; it was assumed that the ultimate capacity of damaged tubular member is reached when the compressive stress in the steel tube at the dent equals the yield stress. The damaged member was treated as a beam-column with uniform cross-sectional properties represented by the dented region. The total eccentricity was taken as the sum of eccentricities due to initial out-of-straightness, external load, and the distance between the original center of the tube and the centroid of the transformed cross section at the dent. Comparing the analytical results with the limited experimental results existent at the time, Parsanejad reported good agreement: the analytical results presented close lower-bound estimates of test results. The equations developed for grout repaired tubulars by Parsanejad has been integrated in ULSLEA and are listed on pages 30-32.

Loh's Interaction Equations for Dent-Damaged Tubulars (Loh, 1993):

Notations

A_d	effective cross-sectional area of dent section
A_0	cross-sectional area of undamaged member
A_{st}	cross-sectional area of the steel
A_s	cross-sectional area of the soil plug in pile
D	outside diameter of tubular member
dd	dent depth
ΔY	primary out-of-straightness of a dented member
ΔY_0	$=0.001 L$
E	Young's modulus
f_y	yield stress
I_d	effective moment of inertia of dent cross-section
I_0	moment of inertia of undamaged cross-section
K_0	effective length factor of undamaged member
K	effective buckling length factor
L	unbraced member length
λ	slenderness ratio
λ_d	slenderness parameter of a dented member $= (P_{ud}/P_{Ed})^{0.5}$
M_u	ultimate moment capacity
M_{cr}	critical moment capacity (local buckling)
M_p	plastic moment capacity of undamaged member
M_{ud}	ultimate negative moment capacity of dent section
M^-	negative moment for dent section
M^+	positive moment for dent section
M^*	neutral moment for dent section
P_{crd}	critical axial buckling capacity of a dented member ($\Delta/L > 0.001$)
P_{crd0}	critical axial buckling capacity of a dented member ($\Delta/L = 0.001$)
P_E	Euler load of undamaged member
P_u	axial compression capacity
P_{ud}	axial compression capacity of a short dented member
P_{crl}	axial local buckling capacity
P_{cr}	axial column buckling capacity
P_v	tensile capacity
r	radius of gyration
t	member wall thickness
UC	unity check

Undamaged Cross Sectional Capacities

$$P_u = F_y A_g \quad \text{for} \quad \frac{D}{t} \leq 60 \quad (2.3.4.23)$$

$$P_u = F_y A_g \left[1.64 - 0.23 \left(\frac{D}{t} \right)^{0.25} \right] \quad \text{for} \quad \frac{D}{t} \geq 60 \quad (2.3.4.24)$$

$$\frac{M_u}{M_p} = 1.0 \quad \text{for} \quad 0 \leq \frac{F_y D}{t} \leq 1500 (\text{ksi}) \quad (2.3.4.25)$$

$$\frac{M_u}{M_p} = 1.13 - 2.58 \frac{F_y D}{E t} \quad \text{for} \quad 1500 \leq \frac{F_y D}{t} \leq 3000 \quad (2.3.4.26)$$

$$\frac{M_u}{M_p} = 0.94 - 0.76 \frac{F_y D}{E t} \quad \text{for} \quad 3000 \leq \frac{F_y D}{t} \leq 300 F_y \quad (2.3.4.27)$$

$$M_p = F_y t (D - t)^2 \quad (2.3.4.28)$$

Dent-Section Properties

$$\frac{P_{ud}}{P_u} = \frac{A_u}{A_g} = \exp \left(-0.08 \frac{dd}{t} \right) \geq 0.45 \quad (2.3.4.29)$$

$$\frac{M_{ud}}{M_u} = \frac{I_u}{I_g} = \exp \left(-0.06 \frac{dd}{t} \right) \geq 0.55 \quad (2.3.4.30)$$

Strength Check

$$UC = \frac{P}{P_{ud}} + \sqrt{\left(\frac{M^-}{M_{ud}} \right)^2 + \left(\frac{M^*}{M_u} \right)^2} \leq 1.0 \quad (2.3.4.31)$$

$$UC = \frac{P}{P_{ud}} + \sqrt{\left(\frac{M^+}{M_u} \right)^2 + \left(\frac{M^*}{M_u} \right)^2} \leq 1.0 \quad (2.3.4.32)$$

Stability Check

$$UC = \frac{P}{P_{crd}} + \sqrt{\left(\frac{M_-}{\left(1 - \frac{P}{P_{Ed}}\right) M_{ud}} \right)^\alpha + \left(\frac{M^*}{\left(1 - \frac{P}{P_E}\right) M_u} \right)^2} \leq 1.0 \quad (2.3.4.33)$$

$$UC = \frac{P}{P_{crd}} + \sqrt{\left(\frac{M_+}{\left(1 - \frac{P}{P_{Ed}}\right) M_{ud}} \right)^2 + \left(\frac{M^*}{\left(1 - \frac{P}{P_E}\right) M_u} \right)^2} \leq 1.0 \quad (2.3.4.34)$$

$$\alpha = 2 - 3 dd / D \quad (2.3.4.35)$$

Critical Buckling Capacities

$$P_{crdo} = P_{ud} [1 - 0.25 \lambda_d^2] \quad \text{for} \quad \lambda \leq \sqrt{2} \quad (2.3.4.36)$$

$$P_{crdo} = P_{ud} \frac{1}{\lambda_d^2} = P_{ED} \quad \text{for} \quad \lambda \geq \sqrt{2} \quad (2.3.4.37)$$

$$\frac{P_{crd}}{P_{crd0}} + \frac{P_{crd} \Delta Y}{\left(1 - \frac{P_{crd}}{P_{Ed}}\right) M_{ud}} = 1.0 \quad (2.3.4.38)$$

Parsanejad's Strength Equation for Grout-Filled Tubulars (Parsanejad, 1987):

Notations

A_g	area of grout at the dented section
A_s	area of steel
A_{tr}, A_{tr}^*	transformed areas at the dented and undented cross section
D	mid-thickness diameter
d	depth of dent
E_g	elastic modulus of grout
E_s	elastic modulus of steel
e	external eccentricity of load
e_g	distance between centroid of grout at the dented cross section to the centroid of undented cross section
e_s	distance between centroid of steel at the dented cross section to the centroid of undented cross section
e_t	$= e + \delta + e_{tr}$
e_{tr}	distance between centroid of the dented and undented transformed cross section
I_g	moment of inertia of grout at dented cross section
I_s	moment of inertia of steel at dented cross section
I_{tr}	transformed moment of inertia of dented cross section
k	nondimensionalized parameter $= A_{tr} e_t / Z_{tr}$
l	effective length of member
m	nondimensionalized parameter $= A_{tr} / A_{tr}^*$
n	elastic modular ratio $= E_s / E_g$
P_u	ultimate axial capacity
P_y	full yield capacity $= A_{tr}^* \sigma_y$
r_{tr}	transformed radius of gyration of dented section
t	thickness of tubular member
Z_{tr}	transformed section modulus with respect to the dented side
α	angle shown in fig.
δ	overall bending
λ	reduced slenderness parameter
σ_a	axial stress
σ_b	bending stress
σ_e	Euler buckling stress
σ_u	ultimate axial stress
σ_y	yield stress of steel

$$\left(\frac{\sigma_u}{\sigma_y}\right)^2 - \left(\frac{1+k}{\lambda^2} + m\right)\left(\frac{\sigma_u}{\sigma_y}\right) + \frac{m}{\lambda^2} = 0 \quad (2.3.4.39)$$

$$\lambda = \sqrt{\frac{\sigma_y}{\sigma_r}} = \frac{1}{\pi} \frac{l}{r_r} \sqrt{\frac{\sigma_y}{E_s}} \quad (2.3.4.40)$$

$$k = \frac{A_r e_t}{Z_r} \quad (2.3.4.41)$$

$$m = \frac{A_r}{A_s^*} \quad (2.3.4.42)$$

Cross-Sectional Properties

$$A_r = A_s + \frac{A_s}{n} \quad (2.3.4.43)$$

$$A_s = \pi D t \quad (2.3.4.44)$$

$$A_s = \frac{D^2}{4} (\pi - \alpha + \frac{1}{2} \sin 2\alpha) \quad (2.3.4.45)$$

$$n = \frac{E_s}{E_r} \quad (2.3.4.46)$$

$$\alpha = \cos^{-1} \left(1 - 2 \frac{d}{D} \right) \quad (2.3.4.47)$$

$$e_r = \frac{A_s e_s + \frac{A_s}{n} e_s}{A_r} \quad (2.3.4.48)$$

$$e_s = \frac{D}{2\pi} (\sin \alpha - \alpha \cos \alpha) \quad (2.3.4.49)$$

$$e_s = \frac{(D \sin \alpha)^3}{12 A_s} \quad (2.3.4.50)$$

$$Z_{tr} = \frac{I_{tr}}{D} \cos \alpha + e_{tr} \quad (2.3.4.51)$$

$$r_{tr} = \sqrt{\frac{I_{tr}}{A_{tr}}} \quad (2.3.4.52)$$

$$I_{tr} = I_s + \frac{I_t}{n} + A_s (e_{tr} - e_s)^2 + \frac{A_t}{n} (e_g - e_{tr})^2 \approx I_s + \frac{I_t}{n} \quad (2.3.4.53)$$

$$I_s = \frac{D^3 t}{4} \left[\frac{\pi - \alpha}{2} - \frac{\sin 2\alpha}{4} + \alpha \cos^2 \alpha - \frac{(\sin \alpha - \alpha \cos \alpha)^2}{\pi} \right] \quad (2.3.4.54)$$

$$I_s = \frac{D'}{64} \left[\pi - \alpha + \frac{\sin 4\alpha}{4} \right] - \frac{D' \sin^6 \alpha}{144 A_s} \quad (2.3.4.55)$$

$$A_{tr} = A_s + \frac{\pi D^2}{4n} \quad (2.3.4.56)$$

2.4 Reliability Analysis

The development of a simplified FOSM method to assess the structural reliability of conventional template-type offshore platforms is described in this section. The primary objectives are to identify the potential failure modes and weak-links of the structure and to estimate bounds on the probability of system failure by taking into account the biases and uncertainties associated with loadings and capacities (Figure 2.4.1).

With this in mind, the maximum static force acting on a platform is treated as a function of random variables. Its statistical properties are derived considering the uncertainties associated with environmental conditions, structure conditions, kinematics, and force calculation procedures. The expected capacity of the platform and the uncertainty associated with it are also characterized. The simplified ultimate limit state analysis procedures described in previous sections are utilized to estimate an expected or best estimate capacity of the platform.

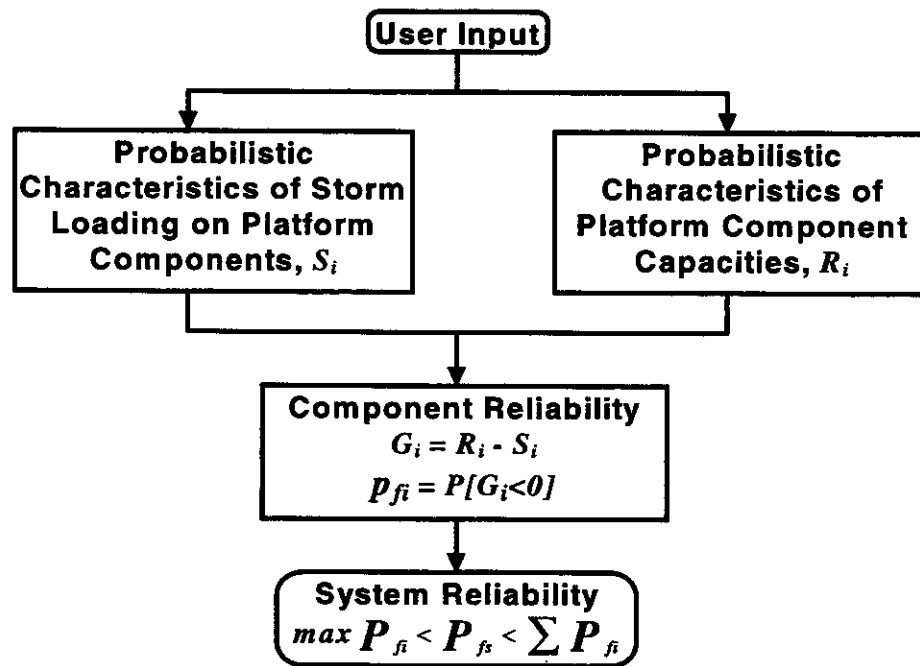


Figure 2.4.1: Probabilistic Failure Analysis

Component Reliability:

The reliability analysis formulated in this chapter is based on the assumption of two-state structural components; a component can be in a safe- or fail-state. Furthermore it is assumed that the uncertainties associated with the state of the component can be described by random variables. For the basic structural component with the resistance R and load S , the probability of failure is equal to the probability that the load exceeds the resistance:

$$p_f = P[R < S] \quad (2.4.1)$$

Based on a mean value first order second moment (MVFOSM) approximation and using the load and capacity equations formulated earlier in this and other chapters, the mean and standard deviation of loads acting on and capacities of platform components can be estimated. Given that the resistance R of a component is a function of random variables (x_1, x_2, \dots, x_n) , its first two statistical moments can be given by:

$$\mu_R \approx R(M_x) \quad (2.4.2)$$

and:

$$\sigma_R^2 \approx \nabla R|_{M_x} \sum \nabla R^T|_{M_x} \quad (2.4.3)$$

where:

$$M_x = [\mu_{x1} \quad \mu_{x2} \quad \dots \quad \mu_{xn}] \quad (2.4.4)$$

is the mean vector of the resistance function and:

$$\sum = \begin{bmatrix} \sigma_{x1}^2 & \rho_{12}\sigma_{x1}\sigma_{x2} & \dots & \rho_{1n}\sigma_{x1}\sigma_{xn} \\ \rho_{21}\sigma_{x2}\sigma_{x1} & \sigma_{x2}^2 & \dots & \rho_{2n}\sigma_{x2}\sigma_{xn} \\ \dots & \dots & \dots & \dots \\ \rho_{n1}\sigma_{xn}\sigma_{x1} & \rho_{n2}\sigma_{xn}\sigma_{x2} & \dots & \sigma_{xn}^2 \end{bmatrix} \quad (2.4.5)$$

defines the covariance matrix, whereas:

$$\nabla R = \left[\frac{\partial R}{\partial x_1} \quad \frac{\partial R}{\partial x_2} \quad \dots \quad \frac{\partial R}{\partial x_n} \right] \quad (2.4.6)$$

is the gradient vector of the resistance function which is evaluated at the mean vector in Equation (2.4.4). The same formulations can be written for the load function S . Defining a safety margin as:

$$M = \ln R - \ln S \quad (2.4.7)$$

the probability of failure can be given by:

$$p_f = CDF(U) \quad (2.4.8)$$

where:

$$U = \frac{(M - \mu_M)}{\sigma_M} \quad (2.4.9)$$

is a standard variate with zero mean and unit standard deviation. μ_M and σ_M are the mean and standard deviation of the safety margin respectively. Presuming lognormal distribution for loads and capacities, the exact reliability index can be given as:

$$\beta = \frac{\mu_M}{\sigma_M} \quad (2.4.10)$$

where:

$$\mu_M = \ln \left(\frac{\mu_R}{\mu_S} \sqrt{\frac{1 + V_S^2}{1 + V_R^2}} \right) \quad (2.4.11)$$

$$\sigma_M^2 = \ln(1 + V_R^2) + \ln(1 + V_S^2) - 2 \ln(1 + \rho_{RS} V_R V_S) \quad (2.4.12)$$

and:

$$P_f = \Phi(-\beta) \quad (2.4.13)$$

where Φ is the cumulative standard normal function. Note that these equations and those derived for jointly normally distributed loads and capacities are the only known exact and closed form solutions of the probability of failure for non-trivial distributions of loads and capacities.

Loading Formulation:

A combination of storm wind load and hydrodynamic wave and current loads is considered:

$$S = S_w + S_h \quad (2.4.14)$$

The wind load is given by:

$$S_w = K_w V_{wd}^2 \quad (2.4.15)$$

where K_w is a structure dependent loading parameter, and V_{wd} is the wind speed that occurs at the same time as the maximum wave height.

The total integrated hydrodynamic drag force acting on a surface piercing vertical cylinder can be expressed as:

$$S_h = K_d K_u H^2 \quad (2.4.16)$$

K_u is an integration function that integrates the velocities along the cylinder and is a function of wave steepness and the wave theory used to estimate the velocities. K_d is a force coefficient and a function of mass density of water ρ , diameter of the cylinder D , and drag coefficient C_d . The mean forces acting on the elements are integrated and the shear force at each component level is calculated. These integrated shear forces define the means of the load variables S_D for deck, S_{ji} for each jacket bay, and the base shear S_F for the foundation bay. The coefficient of variation of the wave load is given as:

$$V_s = \sqrt{V_{K_d}^2 + V_{K_u}^2 + (2V_H)^2} \quad (2.4.17)$$

The dominating storm loading parameters are the maximum wave height and its associated period. An evaluation of the uncertainties in the wind forces does not play a major role and is not included.

Capacity Formulation: Deck Legs' Shear Capacity

A mechanism in the deck leg bay would form when plastic hinges are developed at the top and bottom of all of the deck legs. Using this failure mode as a virtual displacement, virtual work principle can be utilized to estimate the deck leg shear resistance R_d :

$$R_d = \frac{I}{L_d} (2n M_u - Q\Delta) \quad (2.4.18)$$

where:

$$\Delta = M_u L_d \left(\frac{L_d}{6EI} + \frac{1}{C_r} \right) \quad (2.4.19)$$

$$\frac{M_u}{M_{cr}} - \cos \left(\frac{\pi}{2} \frac{Q/n}{P_{crl}} \right) = 0 \quad (2.4.20)$$

The moment capacity of the legs M_{cr} and the local buckling capacity P_{crl} are treated as random variables. Assuming perfect correlation between M_{cr} and P_{crl} , the variance of deck legs capacity can be given as:

$$\sigma_{R_d}^2 = \sigma_{M_{cr}}^2 \left(\frac{\partial R_d}{\partial M_{cr}} \right)^2 + \sigma_{P_{crl}}^2 \left(\frac{\partial R_d}{\partial P_{crl}} \right)^2 + 2\sigma_{M_{cr}}\sigma_{P_{crl}} \left(\frac{\partial R_d}{\partial M_{cr}} \right) \left(\frac{\partial R_d}{\partial P_{crl}} \right) \quad (2.4.21)$$

where $\frac{\partial R_d}{\partial M_{cr}}$ and $\frac{\partial R_d}{\partial P_{crl}}$ are the partial derivatives of the deck legs shear capacity R_d with respect to critical moment and buckling capacities M_{cr} and P_{crl} , evaluated at the mean values $\mu_{M_{cr}}$ and $\mu_{P_{crl}}$.

Capacity Formulation: Jacket Bays' Shear Capacity

Shear capacity in a given jacket bay is assumed to be reached when the vertical diagonal braces are no longer capable of resisting the lateral load acting on the jacket bay. Tensile and compressive capacity of the diagonal braces and the batter component of axial forces in the legs due to overturning moment are included to estimate the jacket bay shear capacity.

It should be noted that the diagonal brace capacities are negatively correlated with the lateral loading. To implicitly account for this correlation, Equation (2.3.2.7) is rewritten in the following format:

$$P_u = \frac{M_u}{8\Delta_o \left(\frac{1}{1 + 2 \frac{\sin 0.5\epsilon}{\sin \epsilon}} \right) \frac{1}{\epsilon^2} \left(\frac{1}{\cos \frac{\epsilon}{2}} - 1 \right)} - \frac{w l^2}{8\Delta_o} \quad (2.4.22)$$

Thus the variance of the compression capacity of a brace can be given by:

$$\sigma_{Pu}^2 = \sigma_{Pcr}^2 + \left(\frac{l^2}{8\Delta_0} \right)^2 \sigma_w^2 \quad (2.4.23)$$

where it is assumed that Δ_0 is a deterministic parameter and that the first term in Equation (2.4.22) equals the buckling load of the brace in the absence of lateral distributed load w :

$$P_{cr} = \frac{M_u}{8\Delta_0 \left(\frac{1}{1 + 2 \frac{\sin 0.5\epsilon}{\sin \epsilon}} \right) \frac{1}{\epsilon^2} \left(\frac{1}{\cos \frac{\epsilon}{2}} - 1 \right)} \quad (2.4.24)$$

To estimate the lateral capacity of a given jacket bay, it is assumed that interconnecting horizontal brace elements are rigid. Thus, the lower-bound capacity of the n^{th} jacket bay R_{Jn} , which is associated with the first member failure in that bay, can be given as:

$$R_{Jn} = \sum_i \bar{\alpha}_n K_i + F_L \quad (2.4.25)$$

where F_L is the sum of batter components of axial pile and leg forces in the given bay and:

$$\bar{\alpha}_n = \frac{P_{u,MLTF}}{K_{MLTF}} \quad (2.4.26)$$

is the lateral drift of the n^{th} jacket bay at the onset of first member failure. K_i are deterministic factors accounting for geometry and relative member stiffness ($\bar{\alpha} K_i =$ horizontal shear force of brace element i at the onset of first brace failure within the given bay). Assuming that there is no correlation between the capacity of the MLTF member and lateral shear in the jacket legs, the variance of the lower-bound capacity of the n^{th} jacket bay can be given as:

$$\sigma_{R_{Jn}}^2 = \left(\sum_i K_i \right)^2 \sigma_{\bar{\alpha}}^2 + B_{F_L}^2 \sigma_{F_L}^2 \quad (2.4.27)$$

where:

$$\sigma_{\alpha} = \frac{\sigma_{Pu,MLTF}}{K_{MLTF}} \quad (2.4.28)$$

B_{FL} denotes the bias associated with the batter component of axial leg forces F_L .

The upper-bound capacity of the n^{th} jacket bay R_{Jn} , which is associated with failure of all main load carrying members in that bay, can be given as:

$$R_{Jn} = \sum_i \alpha_i R_i + F_L \quad (2.4.29)$$

where R_i is the horizontal component of resisting force of the brace element i . α_i account for the post-yielding behavior of semi-brittle brace elements ($\alpha_i R_i$ = residual strength of element i) and are assumed to have deterministic values. Assuming perfect correlation among the member capacities R_i and R_j within the given bay, the variance of the upper-bound capacity of the n^{th} jacket bay can be given as:

$$\sigma_{R_{Jn}}^2 = \sum_{i,j} \alpha_i \alpha_j \sigma_{R_i} \sigma_{R_j} + (B_{FL} \sigma_{F_L})^2 \quad (2.4.30)$$

Capacity Formulation: Foundation

Two basic types of failure mode in the foundation are considered: lateral and axial. The lateral failure mode of the piles is similar to that of the deck legs. In addition to moment resistance of the piles, the lateral support provided by foundation soils and the batter shear component of the piles are considered. The lateral and axial capacity equations for piles in sand and clay are given in Section 2.3.4. These formulations are used to calculate the best estimate capacities. Considering the uncertainties in soil and pile material properties, the uncertainties associated with foundation capacities can also be estimated. However, due to lack of data regarding modeling uncertainties, the total uncertainties associated with axial and lateral pile capacities are assumed to be used, and hence must be supplied by the user. It is intended that user-supplied uncertainties include the uncertainties associated with soil and pile parameters and capacity modeling. The uncertainty associated with the batter component of the pile force is added to the total capacity uncertainty for vertically driven piles.

2.5 Preliminary Design

The preliminary design feature in ULSLEA automatically sizes diagonal braces in a jacket structure, once initial configuration of the jacket has been specified. These properties are selected automatically based on the following ratios:

$D/t = 40$	for braces at top elevations
$D/t = 60$	for braces at bottom elevations
$Kl/r = 70$	for braces at top elevations
$Kl/r = 80$	for braces at bottom elevations

2.6 References

American Petroleum Institute (API), "Recommended Practice for Planning, Designing and Constructing Fixed Offshore Platforms - Load and Resistance Factor Design (RP 2A-LRFD)," First Edition, Washington, D.C, July 1993.

Bea, R.G., DesRoches, R., "Development and Verification of A Simplified Procedure to Estimate the Capacity of Template-Type Platforms," Proceedings, 5th International Symposium Integrity of Offshore Structures, D. Faulkner et al., Emas Scientific Publications, pp. 129-148, 1993.

Fenton, J.D., "A Fifth Order Stokes Theory for Steady Waves," ASCE Journal of Waterway, Port, Coastal and Ocean Engineering, Vol. 111, No. 2, pp. 216-234, 1985.

Focht, J.A., and Kraft, L.M., "Axial Performance and Capacity of Piles," Planning and Design of Fixed Offshore Platforms, McClelland, B., and Reifel, M.D., pp. 763-801, 1986.

Hellan, O., Moan, T., Drange, S.O., "Use of Nonlinear Pushover Analyses in Ultimate Limit State Design and Integrity Assessment of Jacket Structures," Proceedings, 7th International Conference on Behavior of Offshore Structures, Boss '94, Vol. 3, Structures, C. Chryssostomidis (Ed.) Elsevier Science Inc., New York, NY, 1994.

Loh, J.T., "Ultimate Strength of Dented Tubular Steel Members," Proceedings, 3rd International Offshore and Polar Engineering Conference, Vol. 4, pp. 134-145, 1993.

Matlock, H., "Correlations for Design of Laterally Loaded Piles in Soft Clay," Proceedings, Offshore Technology Conference, Houston TX, May 1970.

McDonald, D.T., Bando, K., Bea, R.G., Sobey, R.J., "Near Surface Wave Forces on Horizontal Members and Decks of Offshore Platforms," Final Report, Coastal and Hydraulic Engineering, Dept. of Civil Engineering, University of California at Berkeley, December 1990.

Mortazavi, M., and Bea, R.G., "Screening Methodologies for Use in Platform Assessments and Requalifications," Final Report to Joint Industry-Government Sponsored Project, Marine Technology and Management Group, Department of Civil Engineering, University of California at Berkeley, January 1996.

Parsanejad S., "Strength of Grout-Filled Damaged Tubular Members," Journal of Structural Engineering, ASCE, Vol. 113, No. 3, March 1987.

Randolph, M.F., Houlsby, G.T., "The Limiting Pressure on A Circular Pile Loaded Laterally in Cohesive Soil," *Geotechnique*, London, England, 34(4), pp 613-623, 1984.

Reese, L.C., Cox, W.R., Koop, F.D., "Field Testing and Analysis of Laterally Loaded Piles in Stiff Clay," *Proceedings, Offshore Technology Conference*, Houston TX, May 1975.

Sintef, "USFOS. A Computer Program for Progressive Collapse Analysis of Steel Offshore Structures," Publication N-7034, Trondheim, Norway. Revised Version 6.0, 1994.

Skjelbreia, L., and Hendrickson, J., "Fifth Order Gravity Wave Theory," *Proceedings, 7th Conference of Coastal Engineering*, pp. 184-196, 1961.

Tang, W.H. and Gilbert R.B., "Offshore Lateral Pile Design Reliability," *Research Report for Project PRAC 87-29* sponsored by the American Petroleum Institute, 1990.

Yura, J.A., Zettlemoyer, N., Edwards, F.E., "Ultimate Capacity Equations for Tubular Joints," *Proceedings, Offshore Technology Conference*, OTC 3690, Houston TX, May 1980.

3.0 PROGRAM INSTALLATION

Contents:

3.1	Hardware and Software Requirements	3-2
3.2	Installing ULSLEA	3-2

3.1 Hardware and Software Requirements

The hardware and software requirements for running ULSLEA are:

- An IBM-compatible PC with a 486/66 processor or better, 16 MB internal memory, and 20 MB free hard disk space
- Windows 3.1.1 or Windows 95
- Excel 5.0

Users should refer to Appendix B to check for possible incompatibilities between ULSLEA and other software which may be running.

3.2 Installing ULSLEA

The program diskettes contain the following files:

- ULSLEA.ZIP
- INPUT.ZIP
- EXAMPLE.XLS
- PKUNZIP.EXE

To install the program, do the following:

- In DOS, create an \ULSLEA directory on the target machine and copy the contents of the installation diskettes into the new directory
- Moving to the new directory, use PKUNZIP to unpack the compressed (.ZIP) files. This is accomplished by the following DOS command:

PKUNZIP filename.ZIP

where "filename" refers to the name of the .ZIP file.

The program is now ready to be used. Proceed to the next section for instructions on operating ULSLEA.

4.0 ULSLEA TUTORIAL

This section walks the user through the procedures involved in performing an ULSLEA analysis. In every analysis, the steps will be the same: entering data on environmental conditions and platform configuration through the input screens, and then viewing the output graphically and printed hardcopies. There are no “tricks” or special modeling techniques which must be used with ULSLEA; all input is easily handled by the input preprocessor screens.

Contents:

4.1	Starting the Program	4-1
4.2	Main Menus	4-3
4.3	Inputting Data	4-4
4.3.1	Preliminary Design	4-5
4.3.2	Environmental Conditions	4-5
4.3.3	Global Parameters	4-6
4.3.4	Local Parameters	4-9
	Decklegs and Vertical Diagonal Braces	4-10
	Horizontal Braces	4-12
	Joints	4-12
	Foundation	4-13
	Force Coefficients	4-13
	Boatlandings and Appurtenances	4-14
4.3.5	Member Strength, Material and Soil Properties	4-15
4.3.6	Uncertainties and Biases	4-16
4.4	Calculation	4-17
4.5	Output	4-17
4.6	Saving and Quitting	4-21

4.1 Starting the Program

ULSLEA operates under the MS Windows environment as a visual basic subprogram of MS Excel 5.0. To start ULSLEA, do the following:

- Start MS Excel 5.0
- From the FILE menu in Excel, OPEN the file ULSLEA.XLS

The following menu will appear:

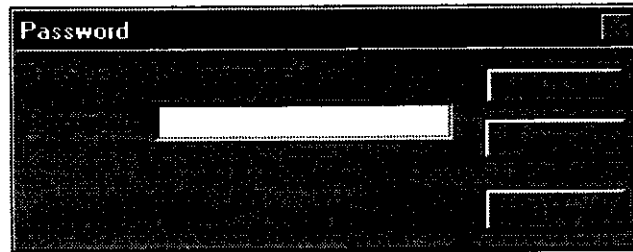


Figure 4.1.1: ULSLEA Password Protection

Enter the ULSLEA password and click OK. Following the loading of the program, a copyright screen will appear:

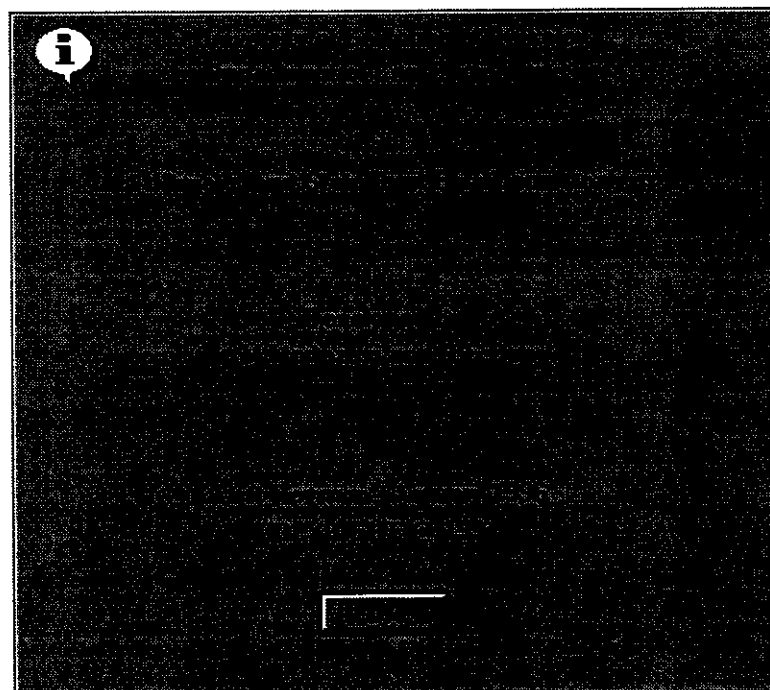


Figure 4.1.2: Copyright Screen

Click OK to acknowledge the version identity. If the program prompts the user at this point to SAVE LARGE CLIPBOARD? the reply should be NO.

Following this, the ULSLEA main menu screen will be displayed and the program is ready for use.

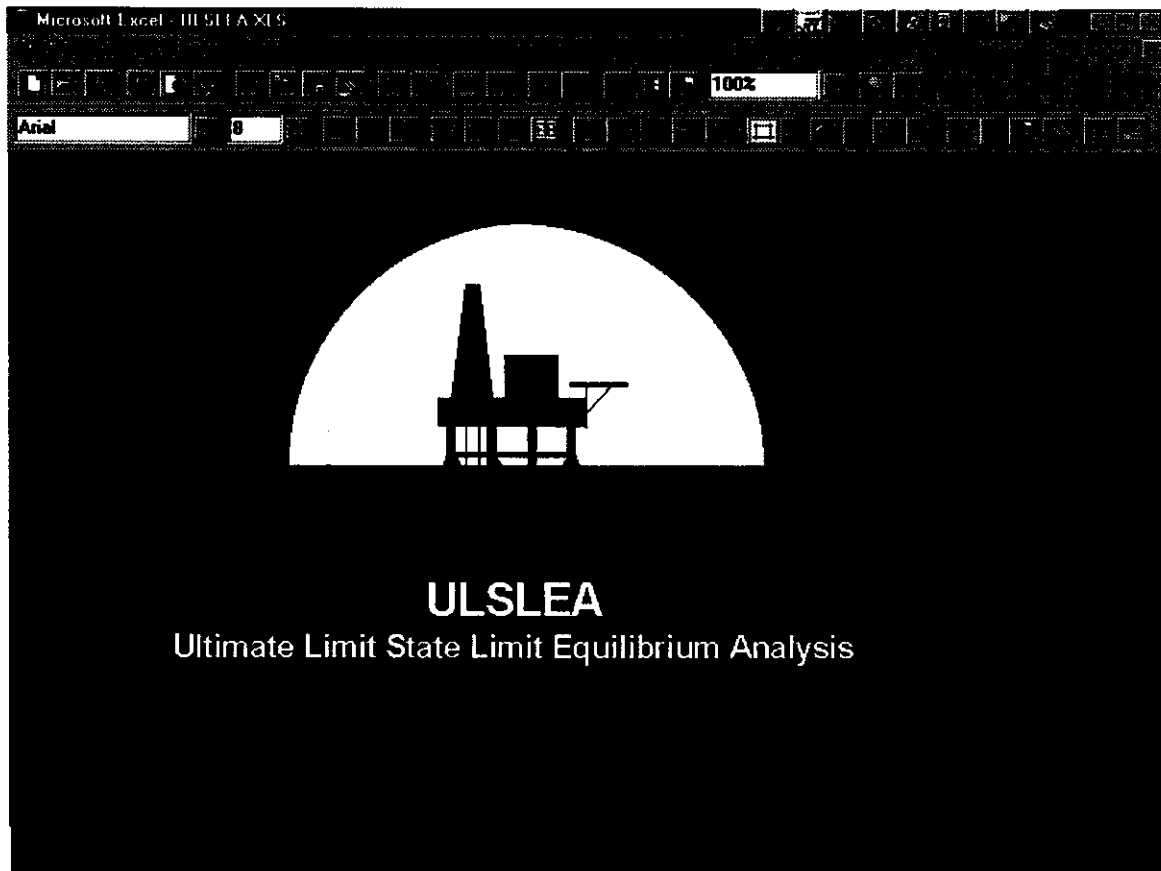


Figure 4.1.3: ULSLEA Main Menu Screen

4.2 Main Menus

There are four main menus for ULSLEA:

- **FILE:** this allows a user to open, close and save data files for the program, as well as to print output.
- **INPUT:** this menu allows the user to input all necessary data for an ULSLEA analysis.
- **CALCULATE:** this menu will allow the user to perform an analysis once all data has been entered.
- **OUTPUT:** this menu will allow the user to view graphical output of the lateral load capacity of the platform for both principle directions, pile axial capacities, and component safety indices.

4.3 Inputting Data

There are two ways of defining input for use in the program:

- by stepping through the INPUT menu and defining the required parameters
- by opening an input file that has been originally created by stepping through the INPUT menu

The INPUT menu contains the following selections:

- Preliminary Design
- Environmental Conditions
- Global Parameters
- Local Parameters (decklegs and vertical braces, horizontal braces, joints, foundation, force coefficients, boatlandings and appurtenances)
- Material and Soil Properties
- Uncertainties and Biases

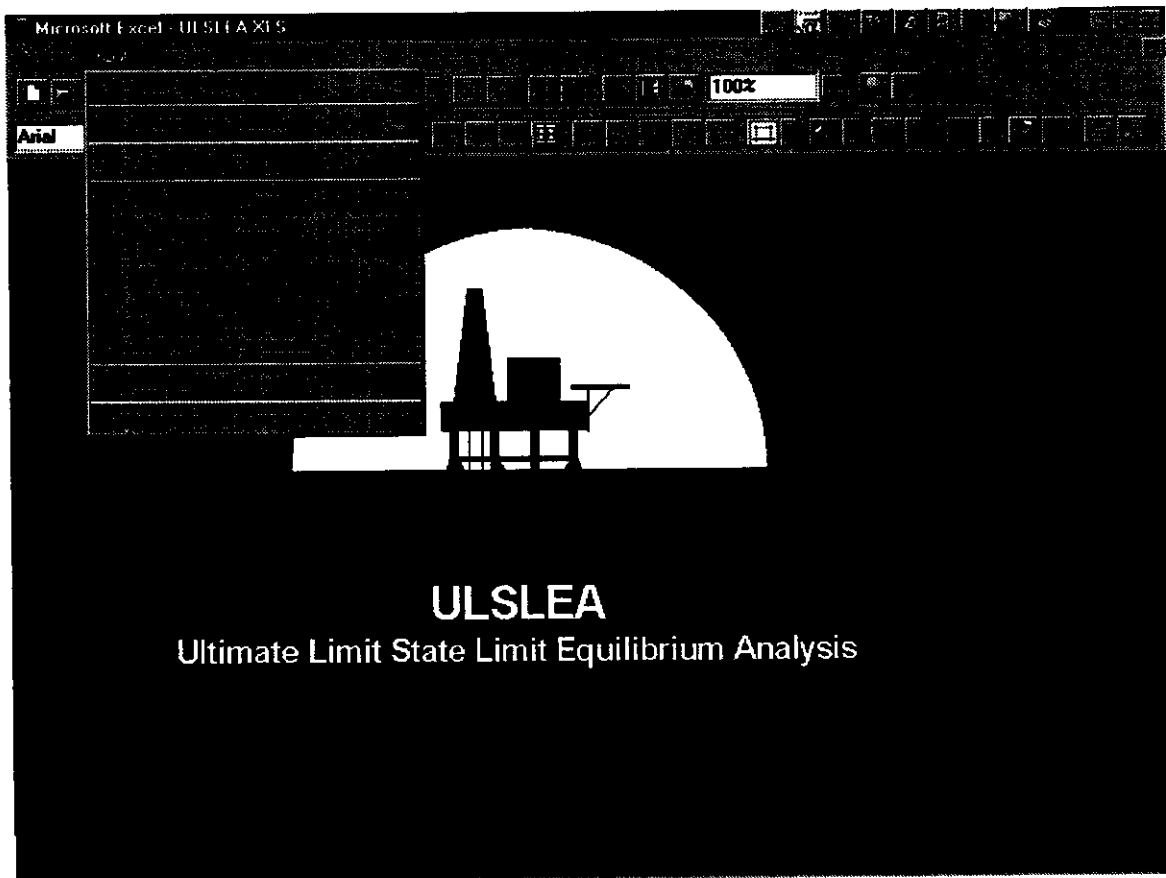


Figure 4.3.1: ULSLEA Input Menu

Each of these selections allows a user to define the relevant environmental and structural characteristics of the platform so that an analysis may be performed. The selections are discussed in detail in the next sections.

4.3.1 Preliminary Design

The preliminary design selection, when selected, will cause the program to automatically size the diameter and thickness of all diagonal braces in the platform. The following will be displayed:

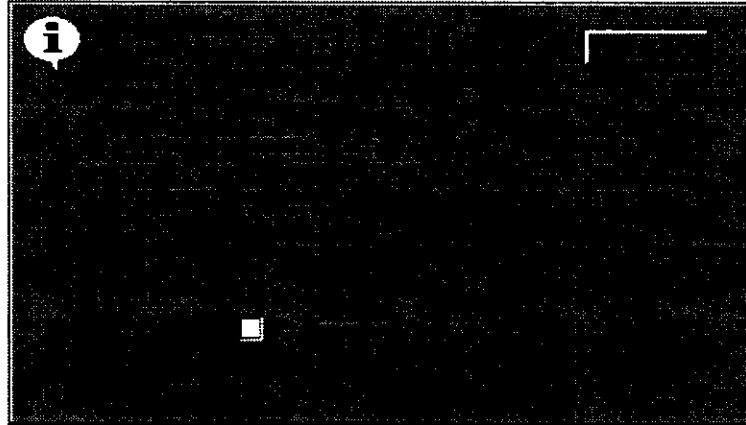


Figure 4.3.1.1: Preliminary Design Screen

The criteria by which these braces are sized is discussed in Section 2.5 of the users manual. This option precludes the need for the user to supply diameter and thickness for diagonal braces when entering information for local parameters (Section 4.3.4). To activate this option, click on the white box, and then click OK.

4.3.2 Environmental Conditions

This selection prompts the user to enter data in order to define the site-specific environmental parameters which are then used to calculate the aero- and hydrodynamic forces acting on the platform. These include water depth, storm surge, wind, wave, and current parameters (Figure 4.3.2.1).

A dark, rectangular window representing a software screen. In the top-left corner, there is a small white circle containing a question mark. The window contains several input fields with numerical values: '213' and '3' in the top right; '125' in a field below them; '66' and '13.5' in fields below that; and '4' and '4' in fields at the bottom. There are also some radio buttons or checkboxes at the bottom left.

Figure 4.3.2: Environmental Conditions

The user may enter data as needed, defining the parameters requested. It should be noted that any combination of wind, waves and current may be used, or each load may be considered individually (i.e. just defining a wave load). When done entering data the user should click OK to save the changes into memory. Clicking CANCEL will leave the data in memory unchanged (or undefined, if no data has been entered).

Note: if linear or quadratic current velocity profiles are specified, the profile is stretched from still water level up to the wave crest so that the water volume remains unchanged. If a constant current velocity profile is specified, the velocities will be equal to the specified velocity everywhere in the water column.

4.3.3 Global Parameters

This selection allows the user to define the global geometry and configuration of the platform being analyzed. The menu for inputting global parameters is shown below in Figure 4.3.3.1:

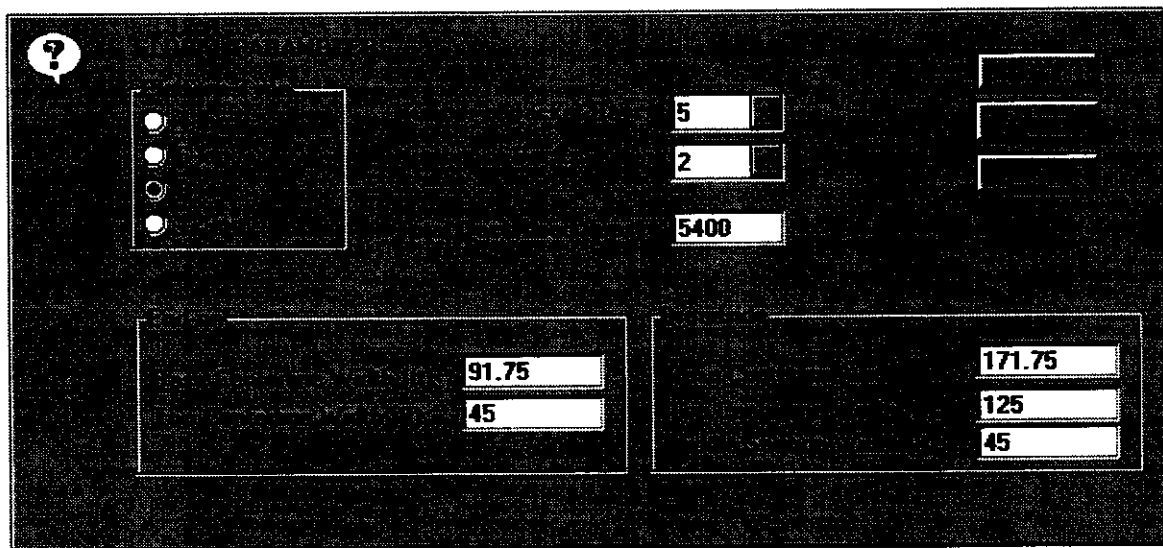
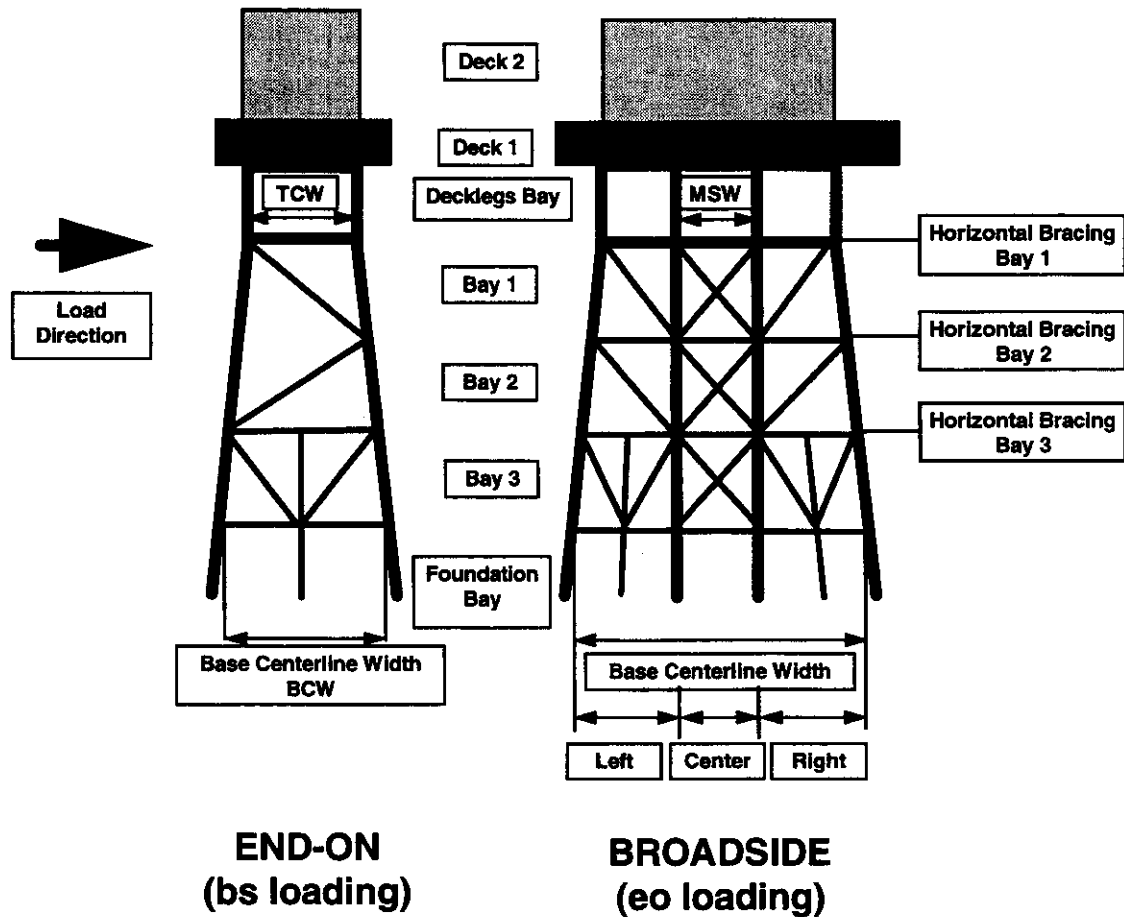


Figure 4.3.3.1: Global Parameters Menu

The input terminology used for entering data is depicted in Figure 4.3.3.2.

The following restrictions apply:

- Number of supporting legs must be 4, 6, 8 or 12, with symmetric pile layout and batter
- Number of jacket bays cannot be greater than 29
- Number of decks cannot be greater than 5.



# of Supporting Legs	# of Decks	# of Jacket Bays
8	2	3

# of Diagonal Braces	End-on	Broadside
Bay 1	4	8
Bay 2	4	8
Bay 3	8	12
# of Skirt Piles	2	4

Figure 4.3.3.2: Input Terminology for Global Parameters

After clicking OK, the user is then prompted to enter the top and bottom elevation (from the SWL), end-on and broadside width, hydrodynamic drag coefficient C_D and wind shape factor C_s for each deck (refer to Figure 4.3.3.3):

40	55	85	125	2.5	1
55	70	65	150	2.5	1

Figure 4.3.3.3: Deck Areas and Force Coefficients

After entering the deck information, the user is then prompted to enter the number of diagonal braces in each jacket bay for both the end-on and broadside elevations (cannot exceed 12 braces for a given bay and elevation), as well as the total number of different joint configurations/sizes for both the end-on and broadside planes (cannot exceed 90 joint configurations).

Note: if it is desired to not include joints as part of an analysis, only one joint should be defined; all diagonal braces would then be indicated as connecting to this single joint type (see Section 4.3.4).

32.5
36
41.5
46.5
51.5
49

4	6
4	6
4	6
4	6
8	6

Figure 4.3.3.4: Bay Heights, Joint and Diagonal Brace Totals

4.3.4 Local Parameters

Information must be supplied regarding the following elements of the platform:

- Decklegs and vertical diagonal braces
- Horizontal braces
- Joints
- Foundation
- Force coefficients
- Boatlanding and appurtenances

Each of these inputs is described in the following subsections. Users should refer to Figures 4.3.4.1A-B for explanation of local parameter terminology regarding diagonal braces, joint types, and horizontal framing:

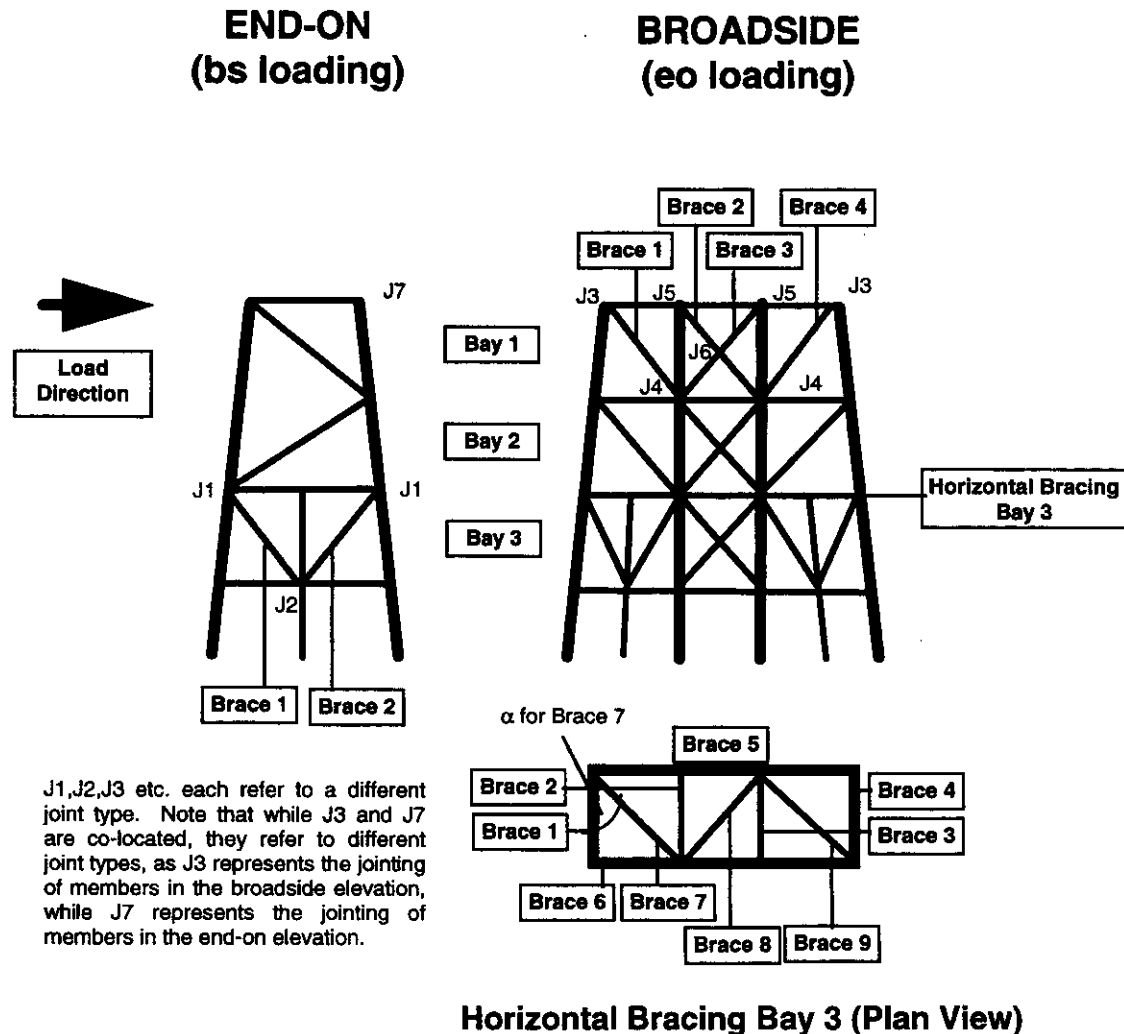


Figure 4.3.4.1A: Bracing Layout

BS Brace #	Type	Position	Configuration	Joint i	Joint j
1	compression	left	S	3	4
2	compression	center	X	5	6
3	tension	center	X	5	6
4	tension	right	S	3	4

EO Brace #	Type	Position	Configuration	Joint i	Joint j
1	compression	-	K	1	2
2	tension	-	K	1	2

Figure 4.3.4.1B: Bracing Information

Decklegs and vertical diagonal braces:

The user is first prompted to input information on the decklegs (Figure 4.3.4.2):

Figure 4.3.4.2: Deck Leg Information

Next, for each jacket bay, the user is prompted for information on the jacket legs and the diagonal braces in each bay for both the end-on and broadside elevations. The box on the right side of the menu may be used to navigate through the different bays and braces. By clicking on “paste data to next brace,” a user may define one brace and then use this option to create a set of duplicates.

Notes:

- If the preliminary design option was selected, brace diameter and thickness does not need to be specified. This will be done automatically.
- For damaged members, the Dent Depth and Out-of-Straightness should be defined. Otherwise, these may be left blank.

- If joints are being excluded from the analysis, and hence only one joint configuration has been defined, joint i and joint j should be the same number.
- When the user is done entering data, “quit” should be selected and then OK.
- This menu will be displayed for every jacket bay in the structure.

?

46

0.5

20

0.5

1

1

Figure 4.3.4.3: Vertical Diagonal Braces Input

Horizontal braces:

For each set of horizontal bracing (see Figures 4.3.3.2 and 4.3.4.1), the user will be prompted for the following information:

14	0.5	45	
14	0.375	45	
14	0.375	45	
14	0.5	45	
12.75	0.5	126	90
12.75	0.5	126	90
18	0.375	61.3	42

Figure 4.3.4.4: Horizontal Bracing Input

The maximum number of horizontal braces in one bay must be no greater than 28. The angle α ($\leq 90^\circ$) is to be measured from an axis parallel to the end-on face of the platform.

Joints:

For each joint that the user wants to include in the analysis, the following input must be provided:

24
0.5
24
45

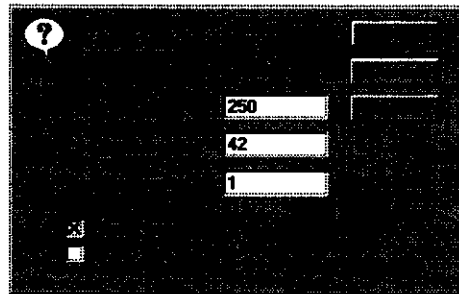
Figure 4.3.4.5: Joint Input

Refer to API RP2A (20th Edition) for joint classifications (K,Y,X). The box to the right may be used to move from joint to joint; also, by activating the paste feature, it is possible to paste information from one joint to the next. This is useful when defining several joints which have similar layout. The branch/chord angle is to be specified in degrees.

Note: if it is desired to exclude joints from the analysis, the user should define only one joint type, and define dummy values for the above inputs.

Foundation:

The following data are to be specified for the main and skirt piles:



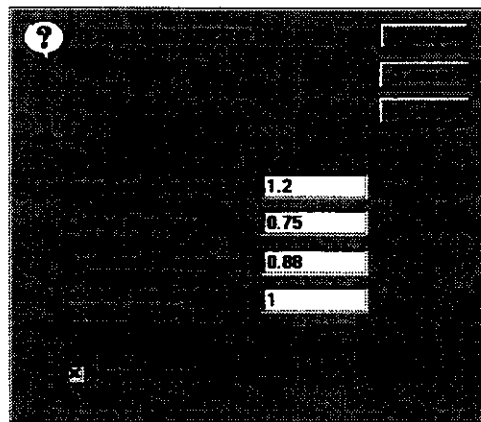
250
42
1

Figure 4.3.4.6: Foundation Pile Input

If it is desired to exclude foundation evaluation from the analysis, dummy input may be supplied here.

Force Coefficients:

The user is prompted to supply the following information:



1.2
0.75
0.88
1

Figure 4.3.4.7: Force Coefficients

If the marine growth box is checked, the user will be asked to supply the amount of marine growth at each level of the structure:

?

MARINE GROWTH

1.5

1.5

1.5

1.5

1.5

Figure 4.3.4.8: Marine Growth

Note: this marine growth is not included in calculating the areas of exposure for boat landings and appurtenances; these items must have marine growth effects included in their estimated effective area (see Section 4.3.4.5).

Boatlanding and Appurtenances:

An equivalent area (ft^2) for boatlanding is to be defined for both end-on and broadside directions. This area is assumed to be at mean water level. An equivalent diameter (ft) for appurtenances (conductors, risers, etc.) is to be defined for deck bay and every jacket bay. The user has to include marine growth thickness when estimating the equivalent diameter for appurtenances, as this is not included by the program.

Figure 4.3.4.9: Boatlanding and Appurtenance Areas

4.3.5 Member Strength, Material and Soil Properties

The user must specify the following material and soil properties:

Figure 4.3.5.1: Member Strength, Material and Soil Properties

Note: at present only one soil layer can be considered.

4.3.6 Uncertainties and Biases

ULSLEA includes a simplified first order second moment reliability analysis (FOSM) subroutine. Failure of each component is defined as the “lower-bound” capacity of the component being reached. The resulting reliability indices are conditional on the specified environmental conditions (storm surge, wave, current, and wind). If reliability analysis is desired, or if biases for a deterministic analysis are to be used, these coefficients should be defined as follows:

1	1
1	0.7

1	0.1
2	0.2
3	0.5
1	0.2
1	0.5
1	0.2

Figure 4.3.6.1: Uncertainties and Biases

Notes:

- The default bias of 0.9 for the jacket load is a modeling bias, which is based on the verification study results. This bias takes into account the conservatism that is introduced by using the simplified load calculation procedure.
- The bias and COV of the strength capacity of tubular braces may be changed to represent degradation due to fatigue, corrosion, or material defects.
- At this point, the COV associated with joint capacity is not included in the reliability analysis
- Bias and COV of axial and lateral pile capacities in sand and clay may be assigned to account for uncertainties in the soil conditions, or for taking into account dynamic loading of the piles.
- Default values of $B = 1.0$ and $COV = 0.10$ are selected for the moment capacity of the decklegs.

- All bias factors are also used in deterministic analysis procedures to predict “best estimate” component capacities and loads acting on these components. The default value for these biases is taken to be $B=1.0$ (except for jacket loads where $B = 0.9$).

4.4 Calculation

When all necessary input has been entered, the user should access the calculation menu and select RUN. ULSLEA will then perform the analysis.

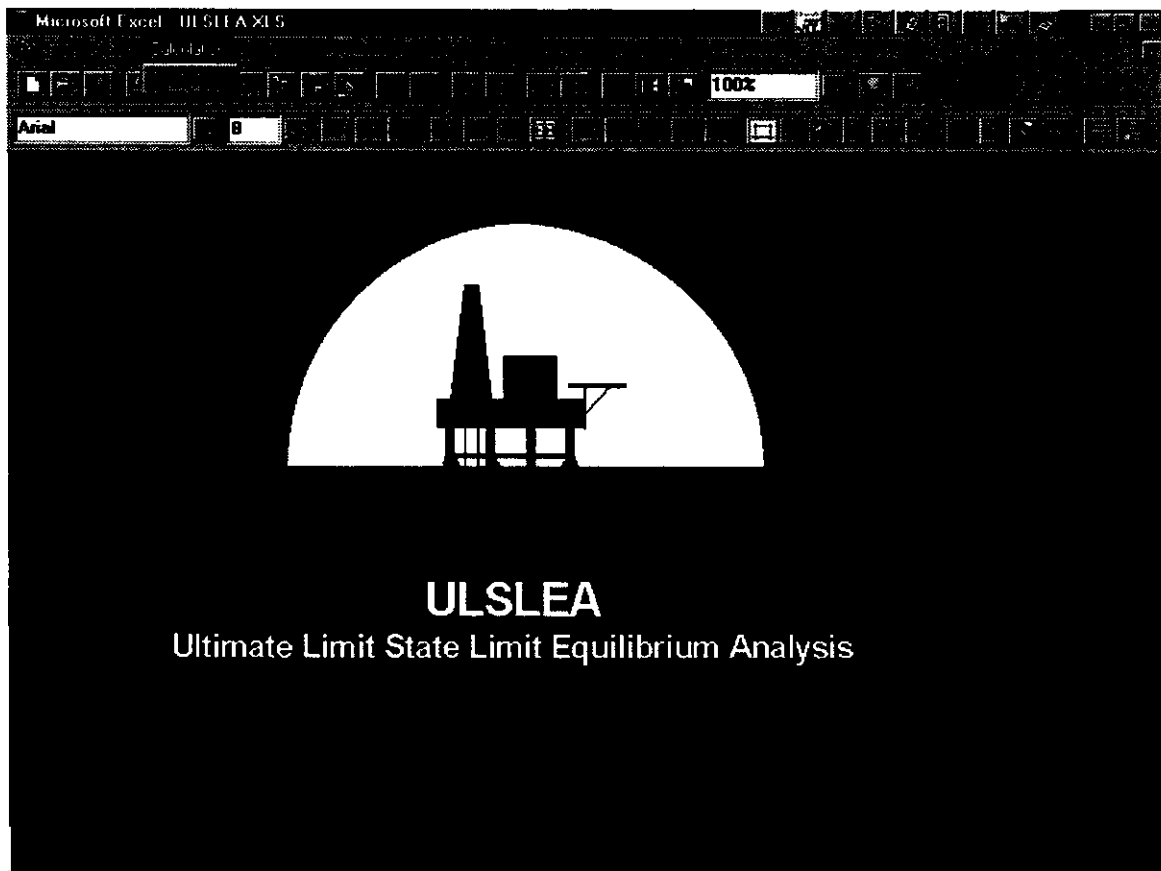


Figure 4.4.1: Calculation Menu

4.5 Output

ULSLEA produces both graphical output as well as printed output summaries. By accessing the Output menu, the user can graphically study the following:

- Cumulative storm shear force and platform's shear capacity vs. platform elevation for both end-on and broadside loading directions
- Kinematics: wave, current, and total velocities vs. platform elevation
- Axial pile performance: $RSR = \text{pile axial capacity/pile axial load}$
- Risk Analysis: conditional component reliability indices for end-on and broadside loading directions

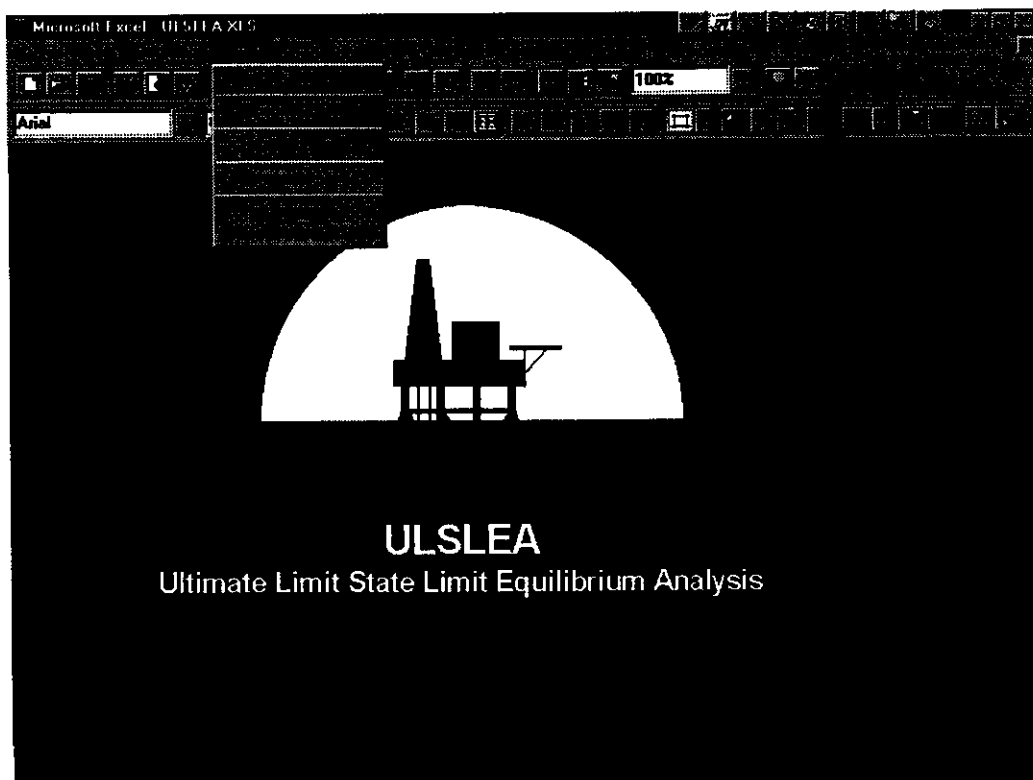


Figure 4.5.1: Output Menu

For the kinematics, the velocity profiles are plotted from mudline to the top of deck legs (bottom of cellar deck). The total velocity is the linear summation of velocities due to current and wave.

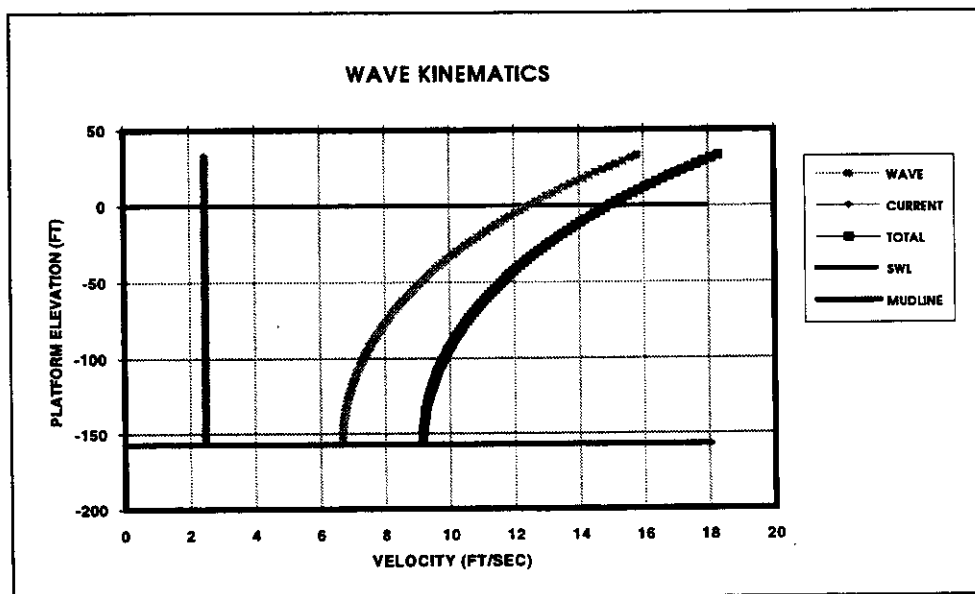


Figure 4.5.2: Kinematics Output

The cumulative storm shear at a given elevation is the integrated wind, wave and current forces acting on the portions of platform above that elevation. The ordinate at the top of the plot (top of the decklegs) corresponds to total wind, wave and current forces acting on the exposed decks of the platform. The ordinate at mudline is the total base shear. When the storm shear profile touches the platform shear capacity profile at any elevation, the corresponding total base shear defines the capacity of the platform. The upper-bound capacity of a given bay is based on failure of all of the load resisting elements. The lower-bound capacity of a given bay is based on first compression member failure and is plotted for jacket bays in addition to the upper-bound capacity. The joint capacity profile is based on first joint failure in each jacket bay.

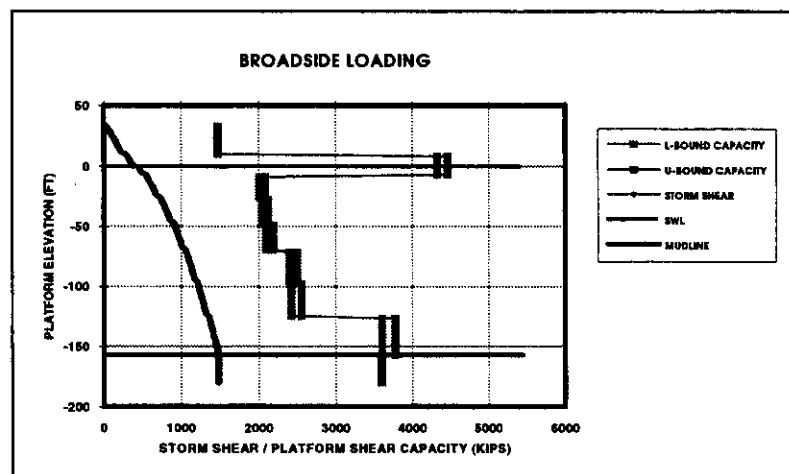


Figure 4.5.3: Storm Shear vs Shear Capacity Output

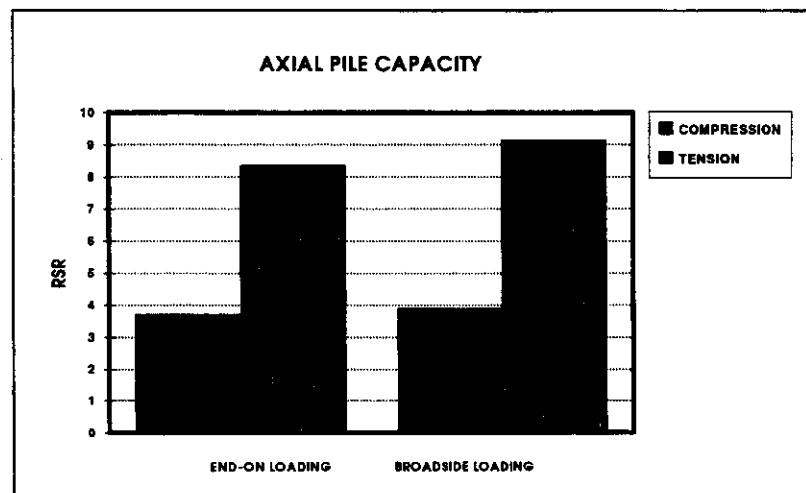


Figure 4.5.4: Axial Pile Performance Output

For each principal orthogonal direction, FOSM reliability indices, β , are plotted for all failure modes. These indices are in general conditional on environmental conditions.

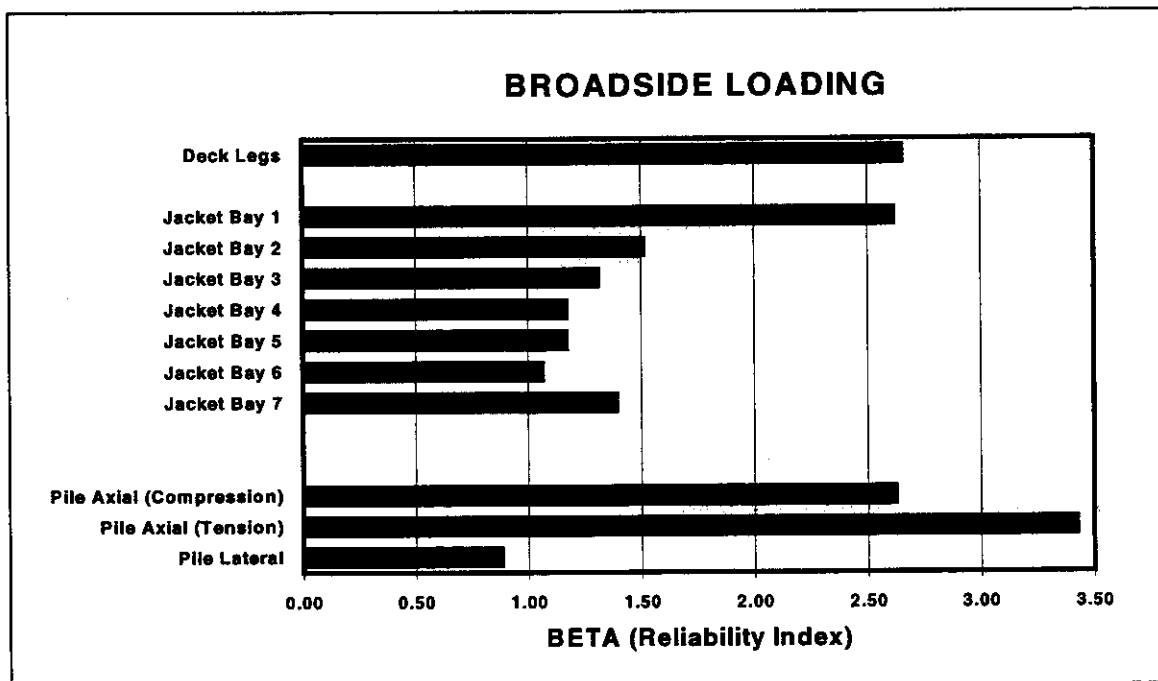


Figure 4.5.5: Risk Analysis Output

In addition to the graphical output, summary tables of the input data may be printed by selecting PRINT from the file menu and then checking the box for input. These tables include an estimate of the steel tonnage of the entire structure, as well as the calculated ultimate axial capacities of the individual diagonal braces in the jacket.

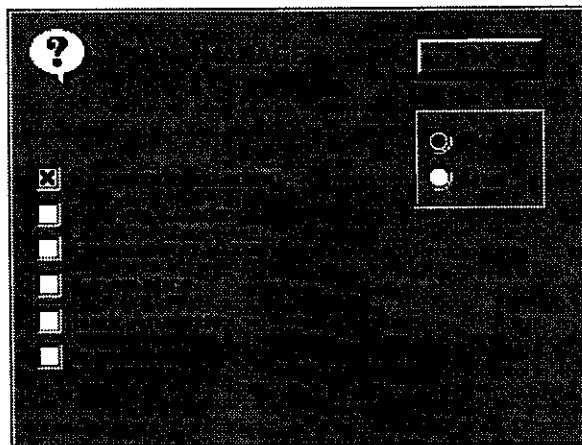


Figure 4.5.6: Printing Selection Menu

4.6 Saving and Quitting

When the analysis is complete, the user should save the input data by accessing the file menu and choosing SAVE. The user will be prompted to give the set of input data a name; this named data file will then be available in the future as a file for additional analysis. The user will always be prompted before quitting to save data:

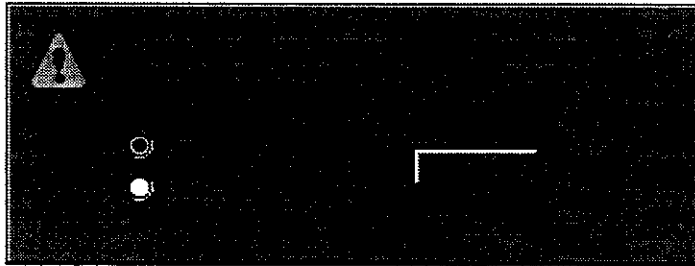


Figure 4.6.1: Save Warning

When through with ULSLEA, the user should again access the file menu, and choose QUIT. If prompted to save changes to the ULSLEA.XLS or INPUT.XLS files when quitting, the user should select NO.

APPENDIX A

Example Application of ULSLEA

Example Platform

The input data and analysis results of a four-leg platform (verification platform C - PMB Benchmark Structure) are included in this appendix. The input file of this 4-leg platform is included on the distribution diskettes under the name "EXAMPLE.XLS". The user can run the analysis of this platform by opening the file ULSLEA.XLS, and choosing EXAMPLE.XLS as the input file.

Users should step through the different input options, in order to familiarize themselves with the input process. The file should be worked through by referencing the steps in the tutorial.

Input Data

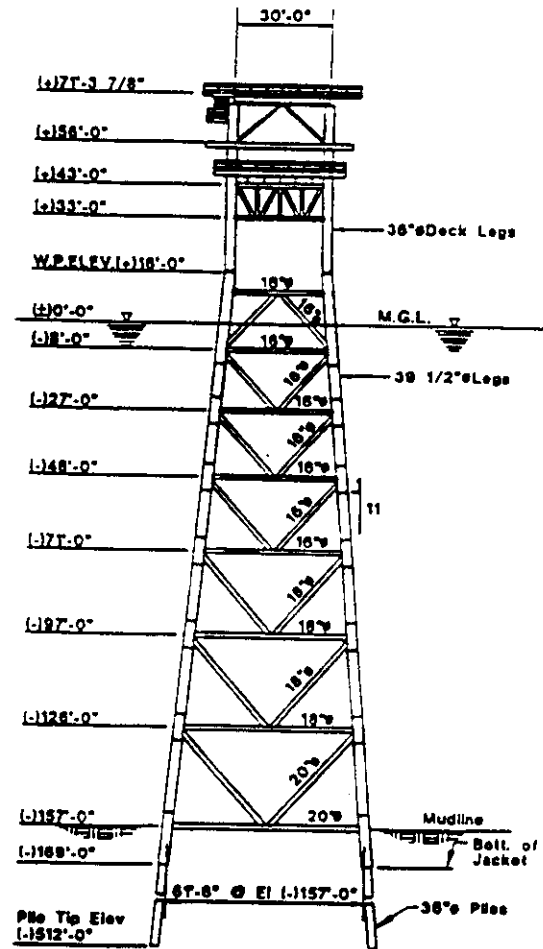


Figure A1: Platform - Typical Elevation (Digre et. al., 1995)

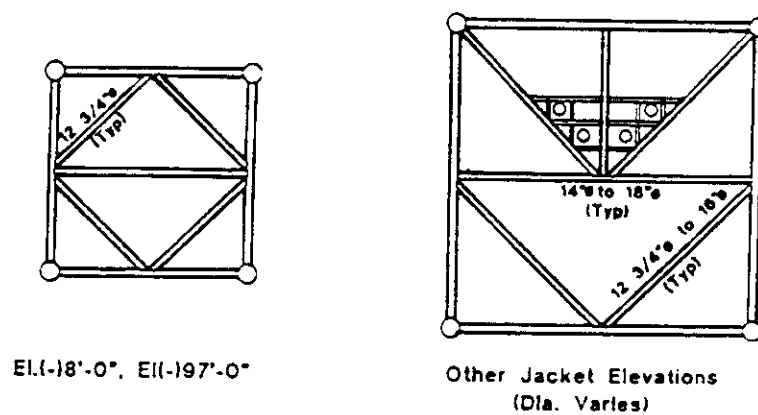


Figure A2: Platform - Typical Horizontal Framings (Digre et. al., 1995)

?

157

3

0

50

14

3.1

3.1

☐

☐

☐

Figure A3: Platform - Environmental Conditions

?

☐

☐

☐

☐

7

4

1742.5

61.5

30

61.5

30

Figure A4: Platform - Global Parameters

33	43	33	33	0.66	
43	56	33	33	2	
56	71	46	46	2.5	
71	86	51	59.75	2.5	

Figure A5: Platform - Deck Areas

?
13

4

4

4

4

4

4

4

4

4

4

4

4

4

4

Figure A6: Platform - Global Parameters

?

36

1

Figure A7: Platform - Local Parameters

?

39.5

1

16

0.843

1

2

Figure A8: Platform - Local Parameters (Vertical Diagonal Braces)

16

0.843

16

47.15

Figure A9: Platform - Local Parameters (Joints)

43

29000

0.65

1

**Figure A10: Platform - Local Parameters
(Member Strength, Material and Soil Properties)**

1.2

2.5

2

0.8

0.88

1

Figure A11: Platform - Local Parameters (Force Coefficients)

1.5

1.5

1.5

1.5

1.5

1.5

1.5

Figure A12: Platform - Local Parameters (Marine Growth)

?

355

36

1.875

☐

☒

Figure A13: Platform - Local Parameters (Foundation)

?

220

220

16.8

16.8

16.8

16.8

16.8

16.8

16.8

16.8

Figure A14: Platform - Local Parameters (Boatlanding and Appurtenances)

16	31.1	90
16	31.1	90
16	31.1	0
16	31.1	0
16	31.1	0
12.75	22	45
12.75	22	45
12.75	22	45
12.75	22	45
12.75	15.6	90

Figure A15: Platform - Local Parameters (Horizontal Bracing - Bay1)

1	1
1	0.7

1	0.1
2	0.2
3	0.5
0.92	0.2
0.9	0.5
0.81	0.21

Figure A16: Platform - Uncertainties and Biases

Output

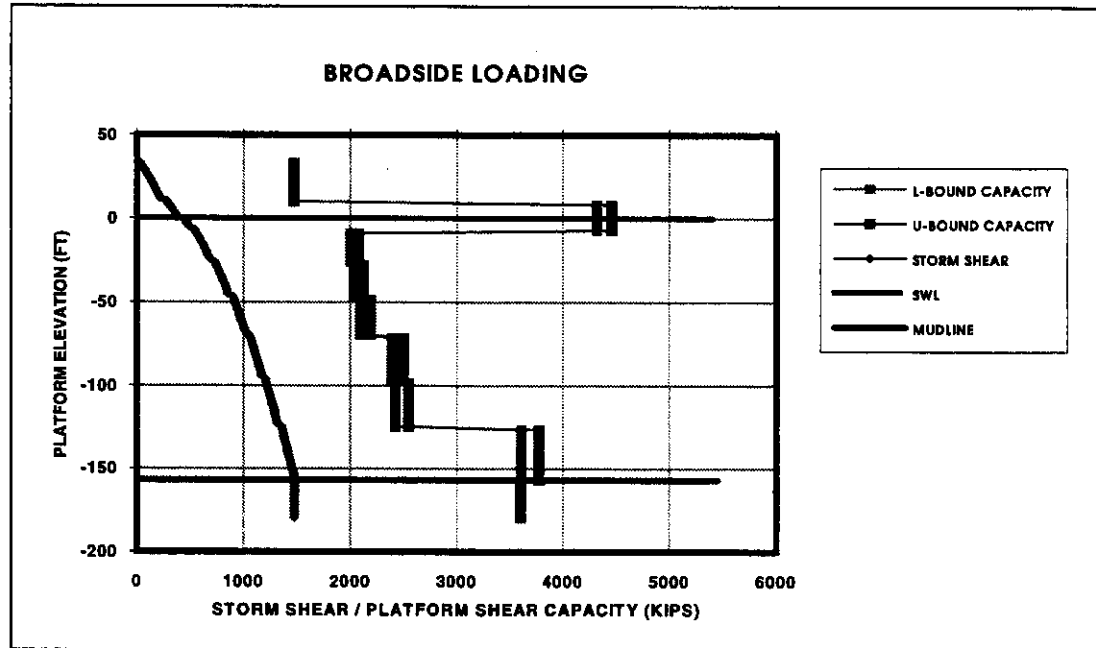


Figure A17: Platform - Storm Shear vs Shear Capacity

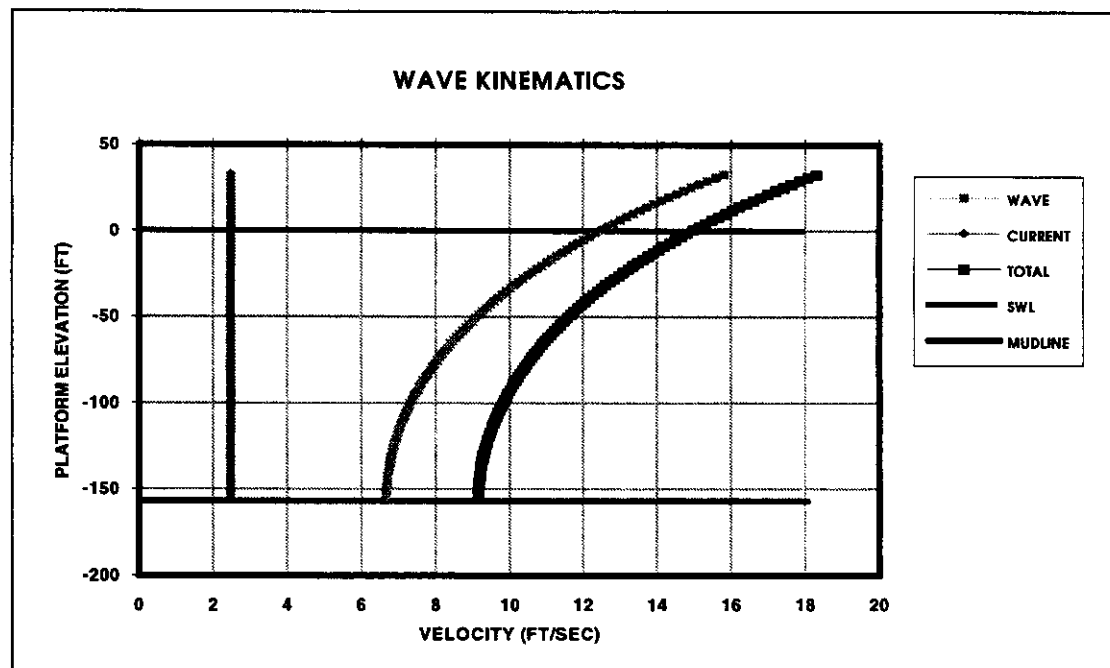


Figure A18: Platform - Kinematics

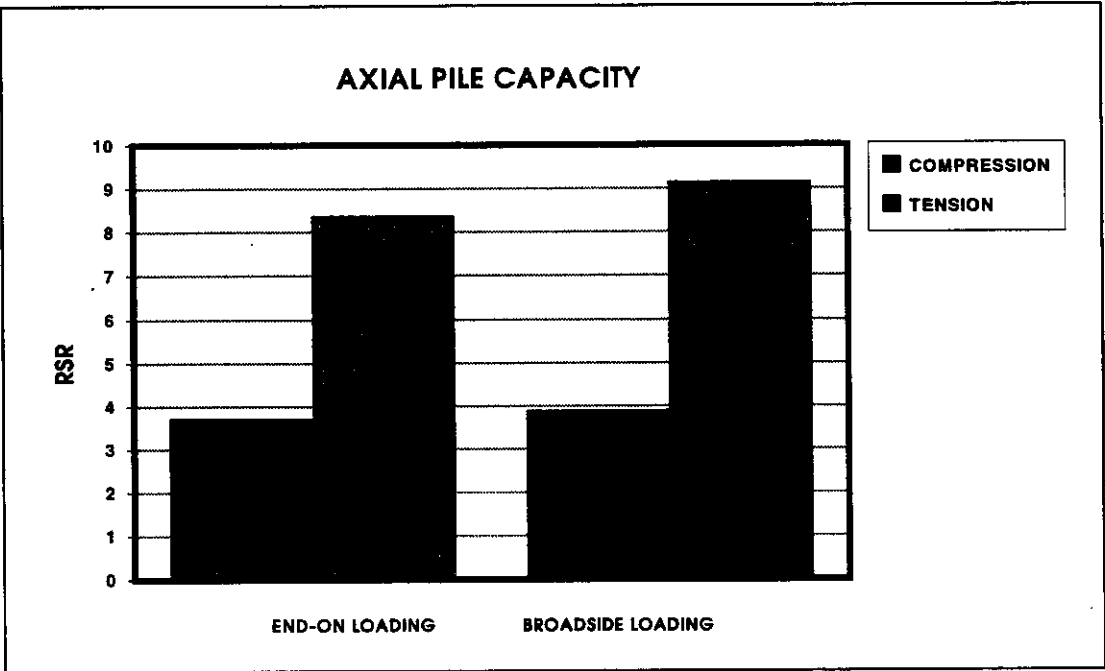


Figure A19: Platform - Axial Pile Performance

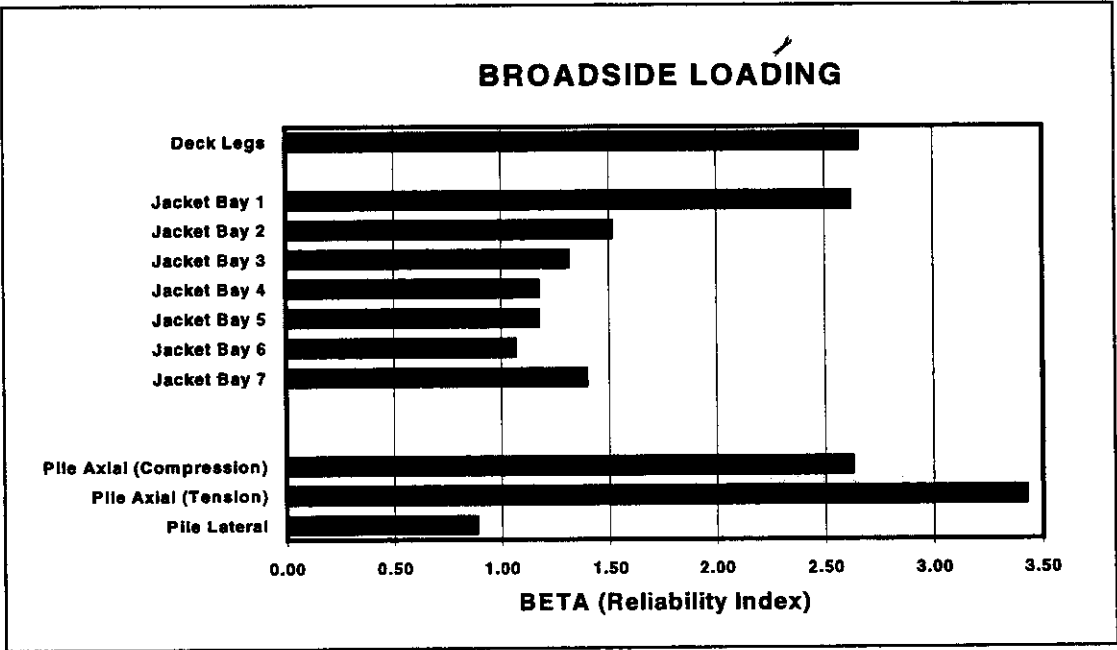


Figure A20: Platform - Risk Analysis (Broadside Loading)

APPENDIX B

Errors and Warnings

Errors and Warnings

This appendix is intended to document errors which are known to exist within ULSLEA, as well as to inform users as to possible problems which may be encountered with ULSLEA due to the operation of other software.

Errors:

- Possible looping error within MS visual basic code (5/1/96). This is being investigated.

Warnings:

- Problems have been encountered running ULSLEA in conjunction with the system program SMARTDRIVE (5/1/96). It is recommended that users who are experiencing long delays with program startup, as well as crashes when attempting to enter data or perform a run, turn SMARTDRIVE off and see if that corrects the problem.
- Problems have been encountered running ULSLEA on versions of Excel 5.0 previous to that which was released with MS OFFICE 4.3 (5/20/96). This problems include crashes associated with attempting to perform a run.